# ARTIFICIAL NEURAL NETWORK (ANN) MODELLING OF HYDROGEN STORAGE IN METAL HYDRIDES

TEE SHU CHING

CHEMICAL ENGINEERING

UNIVERSITI TEKNOLOGI PETRONAS

JANUARY 2021

# Artificial Neural Network (ANN) Modelling of Hydrogen Storage in Metal Hydrides

by

Tee Shu Ching

17000610

Dissertation submitted in partial fulfilment of

the requirements for the

Bachelor of Engineering (Hons)

(Chemical Engineering)

JANUARY 2021

Universiti Teknologi PETRONAS,

32610, Bandar Seri Iskandar,

Perak Darul Ridzuan

CERTIFICATION OF APPROVAL

**Artificial Neural Network (ANN) Modelling of Hydrogen Storage in Metal Hydrides**

by

Tee Shu Ching
17000610

A project dissertation submitted to the
Chemical Engineering Programme
Universiti Teknologi PETRONAS
in partial fulfilment of the requirement for the
BACHELOR OF ENGINEERING (Hons)
(CHEMICAL ENGINEERING)

Approved by,

(Dr Jalal Foroozesh)

UNIVERSITI TEKNOLOGI PETRONAS
BANDAR SERI ISKANDAR, PERAK
January 2021

CERTIFICATION OF ORIGINALITY

This is to certify that I am responsible for the work submitted in this project, that the original work is my own except as specified in the references and acknowledgements, and that the original work contained herein have not been undertaken or done by unspecified sources or persons.

TEE SHU CHING

## ABSTRACT

An artificial neural network (ANN) has been created for the prediction of the hydrogen storage capacity of Mg based alloy hydrides as a function of the alloy composition, pressure and temperature. The aim of this study is to develop an ANN that able to predict the hydrogen storage capacity of Mg based hydrides accurately. In the present study, a total of 103 data were used to develop the ANN model. The architecture of the model consists of one hidden layer with 10 neurons and utilized Hyperbolic Tangent Sigmoid (tansig) transfer function. The neural network is trained using the Levenberg-Marquardt training algorithm. A regression analysis was conducted and showed that the developed model is able to predict accurate hydrogen storage capacity which is indicated by its overall regression coefficient of 0.92767. The neural network used to study the influence of composition of different alloying material, pressure and temperature on the hydrogen storage capacity. For the investigated alloy materials, the hydrogen storage capacity decrease with the increase of alloy composition. The hydrogen storage capacity also increases with the rise of temperature and pressure.

## ACKNOWLEDGEMENTS

First and foremost, I would like to express my deepest and sincere gratitude to my supervisor, Dr Jalal Foroozesh, who is a very passionate educator as he always ensures that I understood the project by providing invaluable guidance and knowledge. I am thankful for his patience and tolerance as the topics of hydrogen storage and artificial neural network modelling are very new to me. His earnest advice and knowledge shared had improved and motivated me to proceed with the project and are greatly appreciated.

My special thanks are extended to the course coordinators of Final Year Project (FYP) I and II, Dr Mohd Hilmi bin Noh and Dr Mohd Dzul Hakim Bin Wirzal for spending their time to inform students the latest updates and helpful information regarding the course throughout my FYP period.

Furthermore, I would like to express my great appreciation to Universiti Teknologi PETRONAS (UTP) for accepting me into the undergraduate program. I am also grateful to the university ITMS staffs for their assistance in providing the MATLAB software for my project.

## TABLE OF CONTENTS


| | | | |
|---|---|---|---|
| **CERTIFICATION OF APPROVAL** | | | **ii** |
| **CERTIFICATION OF ORIGINALITY** | | | **iii** |
| **ABSTRACT** | | | **iv** |
| **ACKNOWLEDGEMENTS** | | | **v** |
| **LIST OF FIGURES** | | | **viii** |
| **LIST OF TABLES** | | | **ix** |
| **LIST OF APPENDICES** | | | **x** |
| **CHAPTER 1:** | **INTRODUCTION** | | 1 |
| | 1.1 | Background | 1 |
| | 1.2 | Problem Statement | 3 |
| | 1.3 | Objectives | 4 |
| | 1.4 | Scopes | 4 |
| **CHAPTER 2:** | **LITERATURE REVIEW** | | 5 |
| | 2.1 | Hydrogen Energy | 5 |
| | 2.2 | Hydrogen Storage Requirement | 7 |
| | 2.3 | Hydrogen Storage | 9 |
| | 2.4 | Magnesium Hydrides as Hydrogen Storage Material | 11 |
| | 2.5 | Alloying of Magnesium Hydrides | 12 |
| **CHAPTER 3:** | **METHODOLOGY** | | 14 |
| | 3.1 | Project Flow | 14 |
| | | 3.1.1 Data Collection | 15 |
| | | 3.1.2 Development of Neural Network | 15 |
| | | 3.1.3 Configure Inputs and Outputs | 17 |
| | | 3.1.4 Initialize the Weights and Biases | 17 |
| | | 3.1.5 Training and Testing of Neural Network | 18 |
| | | 3.1.6 Validation of Neural Network | 19 |
| | | 3.1.7 Improvement and Use of Neural Network | 20 |

**CHAPTER 4: RESULTS AND DISCUSSION** 21

4.1 Optimization of Neural Network Architecture 21

4.1.1 Optimization of Transfer Functions in ANN 21

4.1.2 Optimization of Number of Neurons in ANN 23

4.2 Development of Artificial Neural Network (ANN) 25

4.3 Validation of Neural Network 26

4.4 Analysis of Inputs 28

**CHAPTER 5: CONCLUSION AND RECOMMENDATION** 33

5.1 Conclusion 33

5.2 Recommendation 34

**REFERENCES** 35

**APPENDICES** 41

## LIST OF FIGURES


| | | |
|---|---|---|
| Figure 2.1 | Primary global energy consumption (Rapier, 2020) | 6 |
| Figure 2.2 | Hydrogen stored in gaseous (right) and liquid (left) state (Jain, 2009) | 9 |
| Figure 2.3 | Reaction of a hydrogen molecule with a metal (Dornheim, 2011) | 11 |
| Figure 3.1 | General project work flow | 14 |
| Figure 3.2 | Hydrogen Storage Materials Database Website | 15 |
| Figure 3.3 | MATLAB logo | 16 |
| Figure 3.4 | Inputs and output of the artificial neural network | 17 |
| Figure 4.1 | Flow of input neuron (Dorofki et al., 2012) | 22 |
| Figure 4.2 | MSE values of data versus number of neurons | 24 |
| Figure 4.3 | The architecture of neural network developed | 25 |
| Figure 4.4 | Comparison of predicted outputs and expected outputs | 26 |
| Figure 4.5 | Regression plots and values of ANN | 27 |
| Figure 4.6 | Graph of hydrogen storage capacity (wt%) with varying composition of Mg, Ni, Li, Cu, Al | 29 |
| Figure 4.7 | Graph of hydrogen storage capacity (wt%) with varying composition of Li and Cu in MgNi | 30 |
| Figure 4.8 | Graph of hydrogen storage capacity (wt%) with varying pressure | 31 |
| Figure 4.9 | Graph of hydrogen storage capacity (wt%) with varying temperature | 32 |

## LIST OF TABLES


| | | |
|---|---|---|
| Table 2.1 | Comparison of energy content of fuels (Abe et al., 2019) | 7 |
| Table 2.2 | Overview of some selected parts of the U.S. DOE technical system goals for onboard hydrogen storage for light-duty vehicles (DOE Technical Targets for Onboard Hydrogen Storage for Light-Duty Vehicles \| Department of Energy, n.d.) | 8 |
| Table 3.1 | MATLAB's built-in transfer functions (Al Shamisi et al., 2011) | 18 |
| Table 4.1 | Comparison of transfer functions | 22 |
| Table 4.2 | Comparison between the actual value and predicted value | 29 |

## LIST OF APPENDICES


| | | |
|---|---|---|
| APPENDIX A | Experimental data for model development | 41 |
| APPENDIX B | Milestones of the project | 44 |
| APPENDIX C | Gantt chart of the project | 45 |

# CHAPTER 1

# INTRODUCTION

## 1.1 Background

In the International Energy Outlook 2019 (IEO2019), the U.S. Energy Information Administration (EIA) predicts that consumption of energy worldwide will increase by approximately 50% between the year 2018 and 2050 (Mostyn, 2019). The increase in energy demand maybe due to the rising of income, urbanization and increased access to electricity. Energy can fall into two main categories which are renewable and non-renewable. Currently, 84% of the world's energy are being produced from a non-renewable source which is fossil fuel based on BP's Statistical Review of World Energy 2020 (Rapier, 2020). However, burning fossil fuels to obtain energy has many disadvantages as this activity increases the emission of greenhouse gases which are carbon dioxide (CO2), followed by rising global average temperatures that eventually lead to global warming and causing unprecedented melting of polar sea ice and rising sea levels (Raj & Singh, 2012). This drives further renewable energy development and research to limit the $CO_2$ emission.

Hydrogen, which is the simplest natural element, can be found abundantly in the atmosphere. According to AZoCleantech (2008), the energy content of hydrogen is the highest compared to others common fuel by weight, thus making hydrogen a promising non-polluting energy carrier. Despite its many advantages, the biggest challenge faced is the storage of hydrogen (Jansa et al., 2020; Sang-Kun et al., 2017; Schüth, 2009). Conventional methods on storing hydrogen are either using high pressure to compress the hydrogen or using a low temperature to liquified hydrogen as

hydrogen is an extremely light, low-density gas that tends to strongly repel each other when in molecules form (Zarezadeh Mehrizi et al., 2020). However, these storage methods have many disadvantages such as it uses large volumes in order to store a sufficient amount of fuel, it cannot be stored for a long term and it is unsafe. Therefore, another method of hydrogen storage proposed is by using metal hydrides.

The theory of storing and supplying hydrogen in the form of metal hydrides utilizes the reversible chemical reaction (Yartys et al., 2019). This reaction involves the formation of hydrogen-metal bonds when metal reacts with hydrogen gas and thermal decomposition of the hydride to gain the metal and pure hydrogen back (Dornheim, 2011; Lu et al., 2006). In storing of hydrogen, the hydrogen molecules will break into atomic hydrogen and these will be absorbed in the metallic hydride's lattice under mild conditions - standard room temperatures and atmospheric pressure. This method of hydrogen storage ensures safe storage and reduces the volume required for storing large quantities of hydrogen. Moreover, hydrogen stored in metal hydrides does not have an expiry date as they do not self-discharge.

Magnesium (Mg) has been studied as a potential material to store hydrogen since 50 years ago due to its light weight properties and it is widely available on Earth as Mg is the sixth most abundant metal element in the Earth's crust (Rivard et al., 2019; Webb, 2015; Yartys et al., 2019). Aside from affordability and high abundance, it's high gravimetric hydrogen capacity and energy density which are 7.6 wt% H2 and 13.22 MJ/L respectively place magnesium as a feasible substance to store hydrogen (Mirabile Gattia et al., 2020; Ouyang et al., 2020). However, the practical application of MgH2 in its pure form as a hydrogen storage material has many drawbacks as it is hindered by the high dehydrogenation temperature (above 573 K) and slow adsorption and desorption kinetics, which are caused by high thermal stability and kinetics barrier (Bahou et al., 2020; Peng et al., 2017; Zhang et al., 2017). Studies showed that alloying with other elements can improve the adsorption and desorption kinetics at the expenses of hydrogen storage capacity. Therefore, this project aims to determine the best combination of Mg based alloy hydrides.

## 1.2 Problem Statement

Currently, hydrogen storage is a major obstacle in developing the hydrogen economy. The conventional storage methods like pressurized gas or liquified hydrogen cannot fulfil the storage goals. In order to overcome the hydrogen storage problem, the storage of hydrogen in metal hydrides was proposed. Magnesium (Mg) -based hydrides are chosen as a feasible material for hydrogen storage as it can be found abundantly on Earth, making its cost to be relatively lower compared to other metals. Most importantly, Mg-based hydrides have adequately high hydrogen capacity which is up to 7.6 wt%. However, $MgH_2$ in its pure form is not suitable to be used as hydrogen storage material as it has many drawbacks such as high dehydrogenation temperature (above 573 K) and slow adsorption and desorption kinetics. From the research done, it is determined that the combination of other elements with Mg hydride improved the adsorption and desorption kinetics. Commercial simulators are usually used to study hydrogen storage which they are based on partial differential governing equations but they are computationally expensive and complicated to be used while they are time-consuming. However, there are only limited findings or researches on machine learning of hydrogen storage being performed in spite of the active studies being conducted on materials and structure for hydrogen storage in metal hydride. Therefore, in this project, an artificial neural network model will be present to estimate the best combination of Mg-based alloy hydrides for the performance of storage and the temperature and pressure of hydrogenation.

## 1.3 Objectives

The purpose of this project first and foremost is to fulfil the Final Year Project (FYP) course requirement, where it is mandatory for all final year students to perform research or conduct a project/development in their respective discipline that can overcome real-world problems and produce practical solutions. Students are encouraged to use their available knowledge, techniques and tools to solve the problems encountered and enhancing their skills in applying knowledge and expanding thoughts through managing projects independently.

The objectives of this project are as follow:

- To present a reliable ANN model to predict the performance of hydrogen storage in Magnesium alloy hydrides at different temperature and pressure.
- To offer the optimal composition for the storage using the developed ANN model.

## 1.4 Scopes

This project focuses on the Artificial Neural Network (ANN) modelling of Mg-based alloy hydrides for hydrogen storage at different temperature and pressure. MATLAB software is used to create the model that able to predict the hydrogen storage capacity for Mg-based alloys in this project by entering data collected from the literature review.

# CHAPTER 2

# LITERATURE REVIEW

## 2.1 Hydrogen Energy

In today's world, energy plays a vital part in our daily life. Unfortunately, most people take energy for granted while the energy crisis is on the rise. Energy crisis come from the foreseeable end of the cycle of fossil fuel (*Solutions to the Energy Crisis: How to Achieve Sustainable Energy?*, n.d.). Based on BP's Statistical Review of World Energy 2020, 84% of the world's energy is being generated from fossil fuel such as coal, petroleum, natural gas, and other heavy oils as shown in Figure 2.1 (Rapier, 2020). Fossil fuels are finite meaning that long-run consumption may lead to depletion of resources (Chamoun et al., 2015). However, the energy demand continues to rise as reported by the U.S. Energy Information Administration (EIA) which predicts that the world energy consumption will increase by approximately 50% between the year of 2018 and 2050 in the International Energy Outlook 2019 (Mostyn, 2019). The increase in energy demand and diminishing fossil fuel reserve pose danger to the global energy security. Moreover, burning fossil fuels to obtain energy has many downsides as this activity increases the emission of greenhouse gases, primarily carbon dioxide ($CO_2$) and the global average temperatures which eventually led to global warming and causing unprecedented melting of polar sea ice and rising sea levels (Raj & Singh, 2012). It is supported by *Energy – United Nations Sustainable Development* that stated that 60% of the global greenhouse gas emission is contributed by energy. These reasons encourage renewable energy development which aims to limit the $CO_2$ emission and reduce the current dependence on fossil fuels.

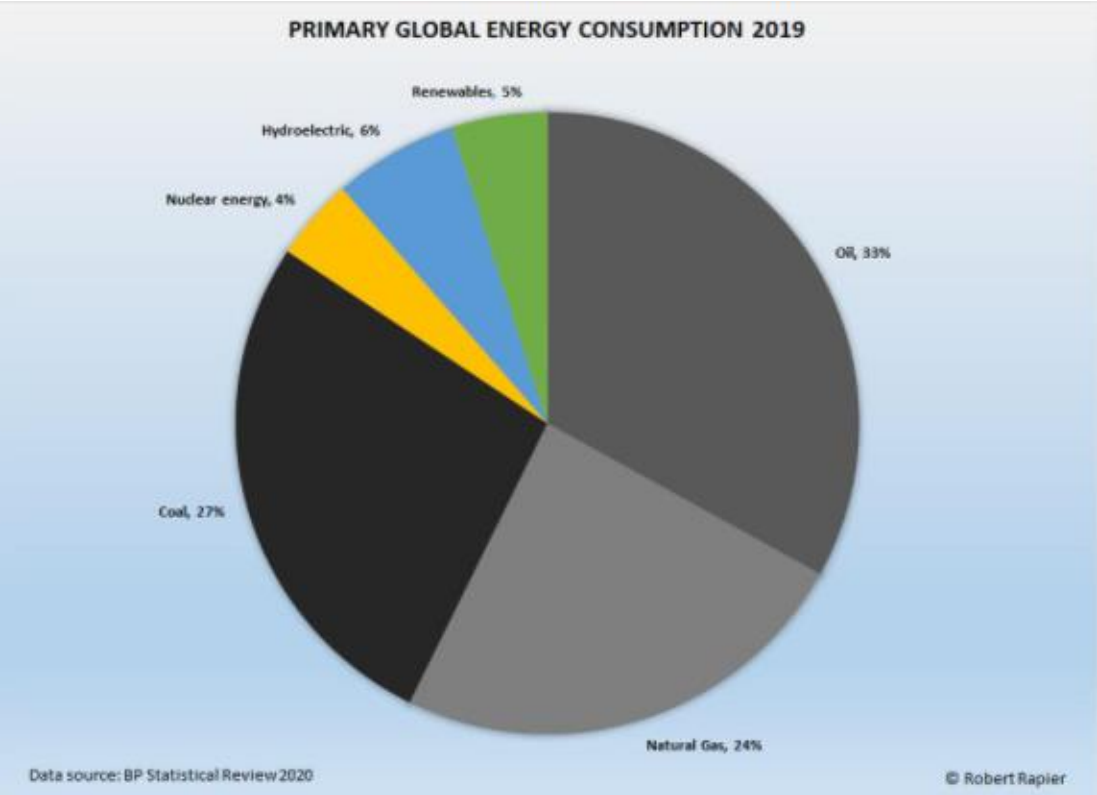


Figure 2.1: Primary global energy consumption (Rapier, 2020)

Hydrogen is highly appraised as a promising non-polluting energy carrier due to hydrogen molecules having these properties. Hydrogen is a non-toxic element that can be found abundantly as it makes up more than 90% of all atoms (Abe et al., 2019). Furthermore, hydrogen molecule has the highest energy content of any common fuel by weight as shown in Table 2.1 while being the lightest element, having a molecular weight of 2.016 (AZoCleantech, 2008; Bellosta von Colbe et al., 2019). Asides from that, hydrogen can be produced from both renewable such as hydro, wind, wave and solar and non-renewable sources such as coal, natural gas and nuclear energy while its waste product is only water when energy is derived from the reaction with oxygen (Montone et al., 2011).

Align with the United Nation's Sustainable Development Goals (SDG) goal 7 which is affordable and clean energy, hydrogen energy can be seen as a sustainable solution to the current energy challenges such as energy security, economic competitiveness and environmental responsibility.

Table 2.1: Comparison of energy content of fuels (Abe et al., 2019)

| Fuel | Energy contents [MJ/kg] | |
|---|---|---|
| | Lower heating value | Higher heating value |
| Gaseous hydrogen | 119.96 | 141.88 |
| Liquid hydrogen | 120.04 | 141.77 |
| Natural gas | 47.13 | 52.21 |
| Liquified Natural Gas (LNG) | 48.62 | 55.19 |
| Still gas (in refineries) | 46.89 | 50.94 |
| Crude oil | 42.68 | 45.53 |
| Liquefied Petroleum Gas (LPG) | 46.60 | 50.14 |
| Conventional gasoline | 43.44 | 46.52 |
| Reformulated or Low-Sulfur Gasoline (RFG) | 42.35 | 45.42 |
| Conventional diesel | 42.78 | 45.76 |
| Low-Sulfur diesel | 42.60 | 45.56 |
| Coal (wet basis) | 22.73 | 23.96 |
| Bituminous coal (wet basis) | 26.12 | 27.26 |
| Coking coal (wet basis) | 28.60 | 29.86 |
| Methanol | 20.09 | 22.88 |
| Ethanol | 26.95 | 29.84 |

## 2.2 Hydrogen Storage Requirement

Despite hydrogen energy having many advantages, the biggest issue faced is the storage of hydrogen (Bellosta von Colbe et al., 2019; Sang-Kun et al., 2017; Schüth, 2009). Regardless of mobile and stationary application hydrogen storage system, both storage systems have their drawbacks. In stationary storage system, weight and volume issues are not as significant when compared to mobile storage system as for stationary application, it can occupy more space, operate at higher temperature and pressure in order to offset the slow kinetics (Abe et al., 2019). On the contrary, hydrogen storage for mobile application has a more exhaustive requirement. The United State DRIVE Partnership which is a partnership between the U.S. Department of Energy (DOE) and the U.S. Council for Automotive Research (USCAR) has summarized the technical performance goals for hydrogen storage systems for onboard light-duty vehicles as in Table 2.2. In Table 2.2, it can be seen that high value of gravimetric and volumetric capacity are highly preferred for hydrogen storage as the gravimetric capacity indicates the quantity of hydrogen that can be stored per weight of the storage tank while the volumetric capacity refers to the amount of hydrogen absorbed per volume of the storage tank.

Table 2.2: Overview of some selected parts of the U.S. DOE technical system goals for onboard hydrogen storage for light-duty vehicles (DOE Technical Targets for Onboard Hydrogen Storage for Light-Duty Vehicles | Department of Energy, n.d.)

| STORAGE PARAMETER | UNITS | 2020 | 2025 | ULTIMATE |
|---|---|---|---|---|
| **System Gravimetric Capacity** | | | | |
| Usable, specific-energy from $H_2$ (net useful energy/max system mass) [b] | kWh/kg (kg $H_2$/kg system) | 1.5 (0.045) | 1.8 (0.055) | 2.2 (0.065) |
| **System Volumetric Capacity** | | | | |
| Usable energy density from $H_2$ (net useful energy/max system volume) [b] | kWh/L (kg $H_2$/L system) | 1.0 (0.030) | 1.3 (0.040) | 1.7 (0.050) |
| **Storage System Cost** | | | | |
| Storage system cost | $/kWh net ($/kg $H_2$) | 10 (333) | 9 (300) | 8 (266) |
| Fuel cost [c] | $/gge at pump | 4 | 4 | 4 |
| **Durability/Operability** | | | | |
| Operating ambient temperature [d] | °C | -40/60 (sun) | -40/60 (sun) | -40/60 (sun) |
| Min/max delivery temperature | °C | -40/85 | -40/85 | -40/85 |
| Operational cycle life (1/4 tank to full) | cycles | 1,500 | 1,500 | 1,500 |
| Min delivery pressure from storage system | bar (abs) | 5 | 5 | 5 |
| Max delivery pressure from storage system | bar (abs) | 12 | 12 | 12 |
| Onboard efficiency [e] | % | 90 | 90 | 90 |
| “Well” to power plant efficiency [f] | % | 60 | 60 | 60 |
| **Charging/Discharging Rates** | | | | |
| System fill time [g] | min | 3–5 | 3–5 | 3–5 |
| Minimum full flow rate (e.g., 1.6 g/s target for 80 kW rated fuel cell power) | (g/s)/kW | 0.02 | 0.02 | 0.02 |
| Average flow rate | (g/s)/kW | 0.004 | 0.004 | 0.004 |
| Start time to full flow (20°C) | s | 5 | 5 | 5 |
| Start time to full flow (-20°C) | s | 15 | 15 | 15 |

Other important hydrogen storage requirements are low pressure and low temperature of hydrogenation (dehydrogenation), low activation energy for charge and discharge of the material, good hydriding (dehydriding) kinetics, long cycle life, high safety under operating conditions and low cost (Malinova & Guo, 2004).

## 2.3 Hydrogen Storage

Hydrogen, which is an extremely light, low-density gas, tends to repel each other strongly when in molecules form making it harder to store them. Based on Malinova & Guo (2004), hydrogen can be stored in three different state – gaseous state, liquid state and solid state. Conventional methods to store hydrogen are in gaseous and liquid states as shown in Figure 2.2. The gaseous state hydrogen storage system is the most well-established storage system in the physical state. In this system, hydrogen is compressed under high pressure between 35Mpa to 70Mpa and is stored as pressurized hydrogen gas (Breeze, 2018; Hua et al., 2011; Krishna et al., 2012). Due to the high pressure, a special storage tank that is made from material that can withstand high pressure such as steel and aluminium is required. On the contrary, liquid hydrogen storage system uses a very low temperature around 20 K or -253$^{o}$C at atmospheric pressure to liquified hydrogen (Andersson & Grönkvist, 2019; Jain, 2009; Yanxing et al., 2019). This low temperature application needed continuous cooling to maintain its liquid state which will increase the operational cost. However, these storage methods have many disadvantages such as it used large volume to store enough fuel, it cannot be stored for a long period and it is unsafe on account of risk of leakage. Therefore, another method of hydrogen storage was proposed is in solid state by using metal hydrides.

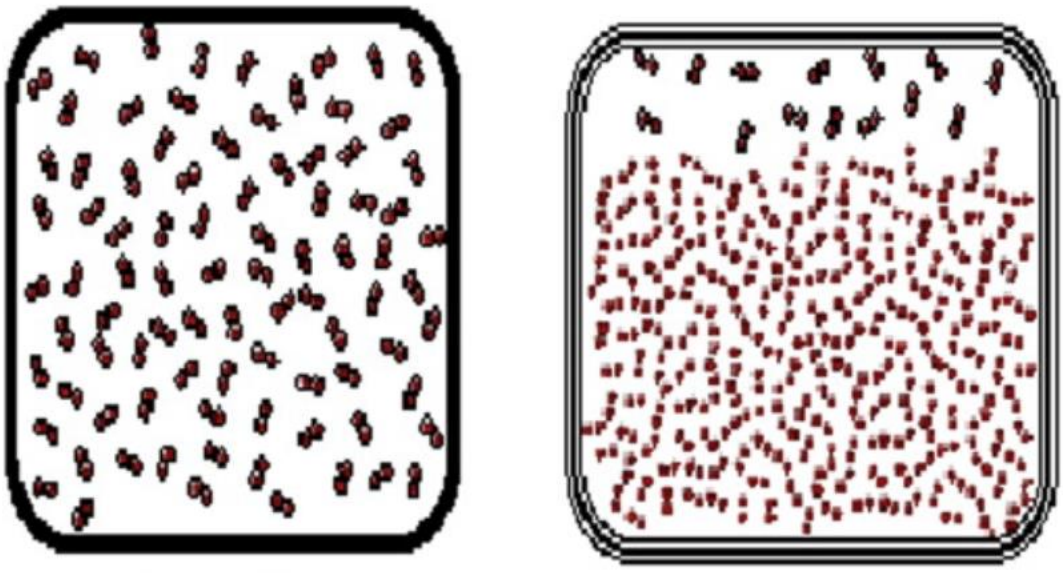

Figure 2.2: Hydrogen stored in gaseous (right) and liquid (left) state (Jain, 2009)

According to Barthelemy et al. (2017), hydrogen storage in solid state provides some advantages in terms of volumetric density compared to storage using high pressure and low temperature. In this project, hydrogen storage in the form of metallic hydrides is focused. The concept of storing and supplying hydrogen in the form of metal hydrides utilizing the reversible chemical reaction is shown as Equation 1 (Abe et al., 2019; Dornheim, 2011).

$$Me + \frac{x}{2} H_2 \leftrightarrow MeH_x + Q \quad (1)$$

Where Me is the solid solution (a metal); $MeH_x$ is the respective hydride; x is the ratio of hydrogen to metal and Q is the heat of reaction. In the formation of metal hydride at ambient and elevated temperatures, the heat of reaction, Q is exothermic where the formation of new bond produces heat that must be released to the surrounding. In contrast, hydrogen desorption or discharge process is an endothermic reaction where the breaking of bonds requires heat from the environment (Dornheim, 2011; Rabienataj Darzi et al., 2016).

According to Dornheim (2011) and Yartys et al. (2019), the reaction of hydrogen with metal is a hetero-phase transformation process where several reaction stages are involved as shown in Figure 2.3. Firstly, the hydrogen molecule is brought to the metal surface where they will have the first attractive interaction. The approaching hydrogen molecule will interact with the surface of metal via Van der Waals force, where the distance between the hydrogen molecule and metal surface is reduced by the power of 6. This will cause them to be in a physiosorbed state. The third step is known as dissociation and chemisorption, where the hydrogen molecule breaks into atomic hydrogen and the newly formed atomic hydrogen will have to overcome activation barrier to form the hydrogen metal bond, leading to become into chemisorbed state. The hydrogen atoms will penetrate the metal surface and diffuse into the bulk lattice to form metal hydride (Dornheim, 2011).

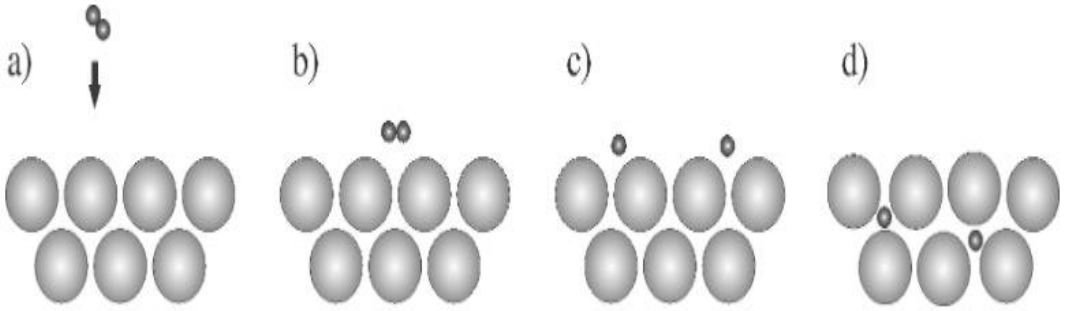


Figure 2.3: Reaction of a hydrogen molecule with a metal (Dornheim, 2011)

Where: a) Transportation of hydrogen molecule to metal surface.

b) Physiosorbed state

c) Dissociation and chemisorption

d) Diffusion into bulk lattice

## 2.4 Magnesium Hydrides as Hydrogen Storage Material

There are many different solid-state hydrogen storage materials such as lithium (Li), aluminium (Al) and boron (B). According to Andersson & Grönkvist (2019), most of the metallic elements able to form binary compounds such as elemental hydrides with hydrogen, but a lot of them are unfitting for hydrogen storage purpose due to thermodynamics, storage capacity or worst scenario, both. Magnesium hydride ($MgH_2$) is considered as propitious elemental metal hydride for large-scale hydrogen storage (Ji et al., 2020; Webb, 2015).

Magnesium (Mg) and magnesium hydride ($MgH_2$) have been investigated intensively as hydrogen storage material since the late 1960s owing to its low cost as it can be obtained by using well-established technology and high volumetric and gravimetric storage capacity which is up to 7.6 wt% and 110g $H_2$/L respectively (Bahou et al., 2020; Sun et al., 2020; Yartys et al., 2019). Asides from that, Mg is a non-toxic material that has high availability as it is the sixth most abundant metal element in the Earth's crust. Furthermore, the operation of Mg in hydrogen storage

application is much safer compared to other light elements (Yartys et al., 2019). More importantly, $MgH_2$ can be synthesized by hydrogenation of magnesium as shown in Equation 2 below with great reversibility (Sasaki et al., 2016; Sun et al., 2020).

$$Mg + H_2 \rightarrow MgH_2 \qquad \Delta H = 76\ kJ/mol \tag{2}$$

## 2.5 Alloying of Magnesium Hydrides

The practical application of $MgH_2$ in its pure form as a hydrogen storage material has many drawbacks as it is hindered by the high dehydrogenation temperature (above 573 K) and slow adsorption and desorption kinetics, which are caused by high thermal stability and kinetics barrier (Bahou et al., 2020; Peng et al., 2017; Zhang et al., 2017). According to Zhang et al. (2017), the hydrogenation process of magnesium hydride is controlled by three steps, namely:

a) Dissociation of hydrogen molecule into atoms on magnesium surface,
b) Diffusion of hydrogen atoms into magnesium's lattice,
c) Formation of $MgH_2$ molecules.

The dissociation of hydrogen molecules is regarded to be the rate-limiting factor on account of the high energy required, which eventually leads to poor kinetics. This is because higher activation energy will cause the reaction to be slower as reactants needed to obtain sufficient energy to become unstable.

A substantial amount of research has been performed to enhance the hydrogen sorption kinetics and reduce dehydrogenation temperature. From the research done, it is determined that combination of other elements such as transition metals and their alloys with magnesium hydride have improved the adsorption and desorption kinetics (Sakintuna et al., 2007; Sun et al., 2020; Wang et al., 2017; Webb, 2015). This statement is further supported by Zhang et al. (2017) who conducted the experiment of alloying Molybdenum disulfide ($MoS_2$), where $MgH_2$ indicated that the compound which the $MoS_2$ is added to had developed a catalytic action on the hydrogen

absorption and further improved the hydrogen sorption kinetics. Additionally, the $MoS_2$ particles are found to provide many pathways for the infiltration of hydrogen and active nucleation sites for the formation of $MgH_2$. Although the addition of other elements play a vital role in improving hydriding kinetics, but, the presence of the added element, in this case, is $MoS_2$ suffers a noticeable decrease in the maximum hydrogen absorption capacity due to the deadweight of $MoS_2$. Therefore, the improvement of hydriding rate is caused by the addition of $MoS_2$ with the cost of capacity loss.

# CHAPTER 3

# METHODOLOGY

## 3.1. Project Flow

According to MATLAB, the work flow for a general neural network consists of 7 primary steps as shown in Figure 3.1.

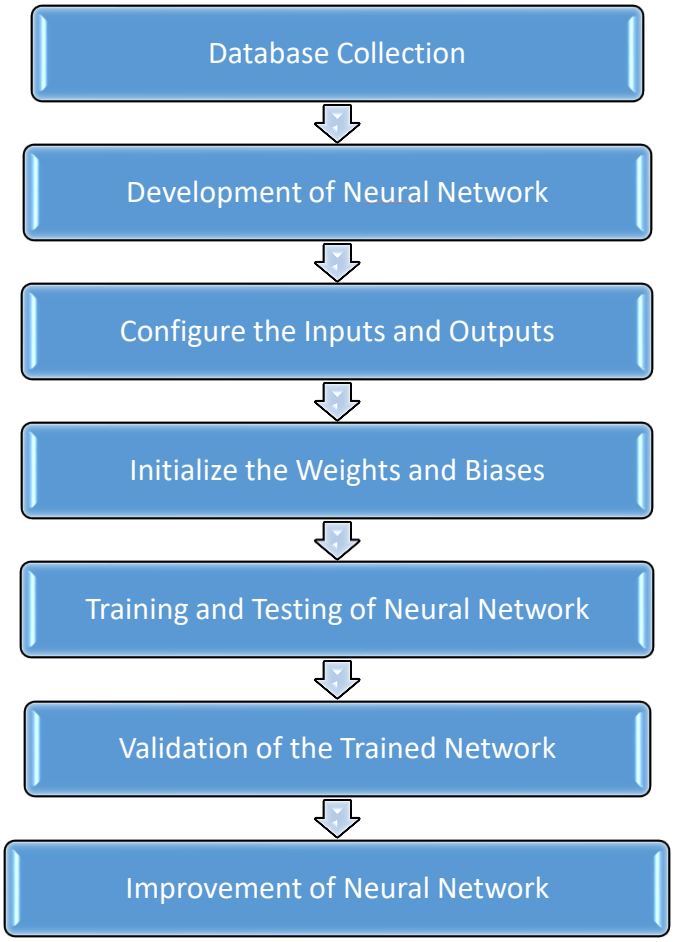


Figure 3.1: General project work flow

### 3.1.1 Data Collection

Data collection is the first step in developing an ANN model. As in this project, a total of 103 data were collected and they are chemical composition of Magnesium (Mg), Nickel (Ni), Copper (Cu), Lithium (Li) and Aluminium (Al) as well as pressure and temperature which are measured in bar and ℃ respectively and Hydrogen Storage Capacity (wt%). This information is obtained from the Hydrogen Storage Materials Database website as shown in Figure 3.2 which was created to retain data from the United State Department of Energy (DOE) Hydrogen Storage funded research. This database is made accessible to all research communities to encourage the development of advanced hydrogen storage materials (Lenahan, 2011).

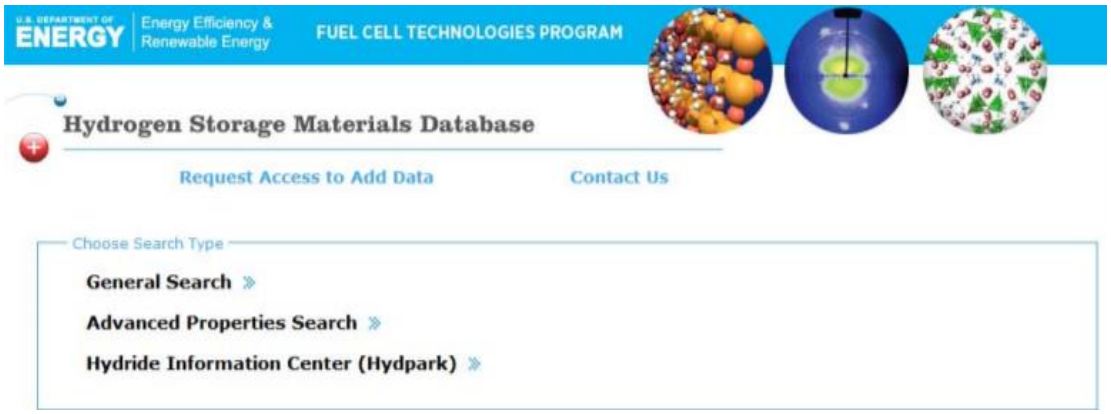


Figure 3.2: Hydrogen Storage Materials Database Website

### 3.1.2 Development of Neural Network

An ANN is a biologically inspired computational network consisting of interconnected processing units, also known as artificial neurons (Anghel et al., 2014). The ANN is designed and developed by using Neural Network Toolbox™ from MATLAB, a computer-aided engineering software. Figure 3.3 shows the MATLAB logo. By using this toolbox, a neural network can be constructed and trained in a less complex way due to the in-built functions that MATLAB provides. Before advancing to the development of neural network, effort and time are invested in learning the Neural Network Toolbox™ by performing research online.

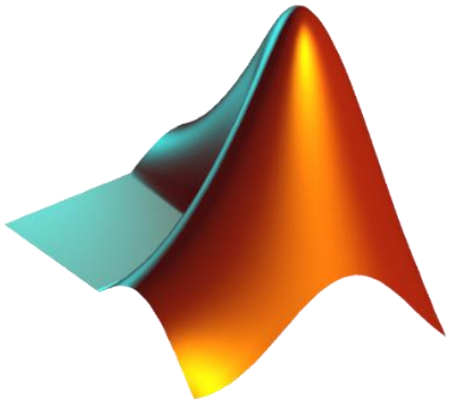

Figure 3.3: MATLAB logo

There are several types of neural networks such as feed forward neural network, modular neural network, Kohonen self organizing neural network, and recurrent neural network. For this dissertation, the feed forward neural network with backpropagation algorithm will be applied. The feed forward network is the most popular and most commonly used model among all artificial neural networks. In the feed forward network, there are different layers: input layer, hidden layer(s) and output layer. In this network, the information moves in one direction which is from the input layer to the hidden layer(s) and last stop at the output layer.

The backpropagation algorithm which is a supervised learning method for the feed forward network works by altering the internal weightings of input signal to generated desired output (Brownlee, 2016). The internal weightings are modified using the error between the generated output and known output. The backpropagation of error is utilized to train the network. In MATLAB's toolbox, there are several built-in training functions such as Levenberg-Marquardt (trainlm), BFGS Quasi-Newton (trainbfg), Scaled Conjugate Gradient (trainscg) and Fletcher-Powell Conjugate Gradient (traincgf). Liu (2010) indicates that Levenberg-Marquardt training algorithm is the most effective method for feed forward neural network with the respect to training precision. Hence, Levenberg-Marquardt training method is selected.

### 3.1.3 Configure Inputs and Outputs

The neural network must be configured after it has been created. The configuration step involves inserting input and target data and setting the sizes of the input and output to match the data. In this project, the inputs and output data are the chemical composition of Magnesium (Mg), Nickel (Ni), Copper (Cu), Lithium (Li), Aluminium (Al), pressure and temperature and hydrogen storage capacity as shown in Figure 3.4. The output data is inserted as the target data.

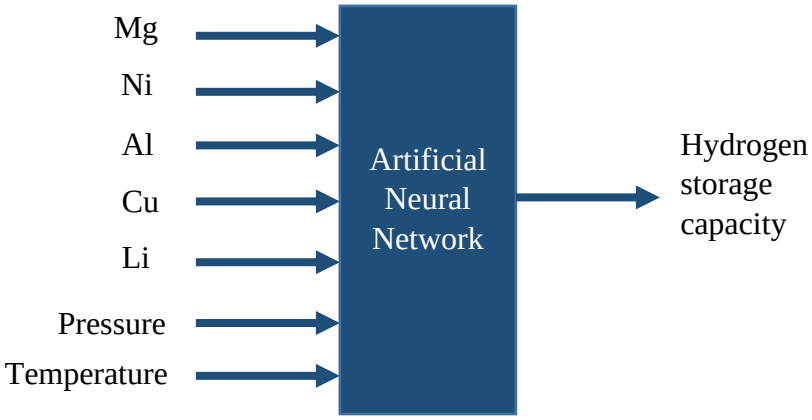


Figure 3.4: Inputs and output of the artificial neural network

As MATLAB read matrix vertically instead of horizontally, it is necessary for the inserted matrix to be transposed to ensure that the size of the inputs and output is similar. The transpose of matrix interchanged the row and column index for each data and reflecting the data across the main diagonal.

### 3.1.4 Initialize the Weights and Biases

Weights and biases, also known w and b, are learnable parameters of ANN. The weights govern the strength of the connection between neurons while the biases are the additional input into the next layer. The biases are constant to ensure that there will be activation in the neurons even when the input is zero. In this project, the weights and biases are generated automatically by the built-in capabilities of MATLAB's Neural Network Toolbox™.

### 3.1.5 Training and Testing of Neural Network

The developed ANN are trained using the data collected in section 3.1.1. The 103 data collected are separated into 3 different groups in the ratio of 70:15:15. The first group which have 70% of total data is used for the training of model while the second and third group is used for validation and testing respectively. The train group of data allows the model to obtain ideal values for parameters such the values of weights and biases. Conversely, the validation set aims to enhance the model's ability to make generalizations and serves to stop the training process when validation error kept increasing for consecutive epochs. Lastly, the test set's purpose is to evaluate the performance of the model by obtaining the unbiased prediction values using the unknown data.

The training process occurs first and followed by the validation process and lastly is the testing process. As it is outlined in section 3.1.2, the training algorithm used is Levenberg-Marquardt algorithm for the feed forward neural network. Besides that, MATLAB provides built-in transfer functions such as linear (purelin), Hyperbolic Tangent Sigmoid (tansig) and Logistic Sigmoid (logsig) to generate output. The transfer function used in this project is tansig as it maintains the learning process even when it generate a value close to -1.0 whereas the logsig's learning rate decrease when the output of hidden neuron close to zero. The Table 3.1 shows the graphical illustration and mathematical form of the transfer functions.

Table 3.1: MATLAB's built-in transfer functions (Al Shamisi et al., 2011)

| Function Name | Graphical Illustration | Mathematical form |
|---|---|---|
| Linear | 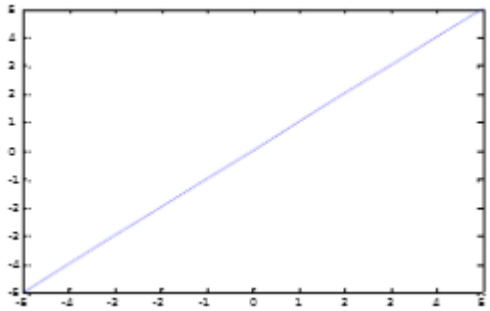 | $f(x) = x$ |

| | | |
|---|---|---|
| Hyperbolic Tangent Sigmoid | 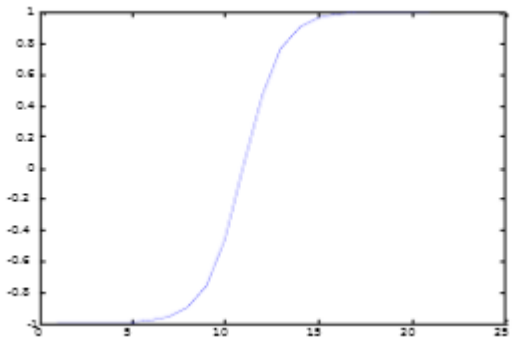 | $f(x) = \frac{e^{x} - e^{-x}}{e^{x} + e^{-x}}$ |
| Logistic Sigmoid | 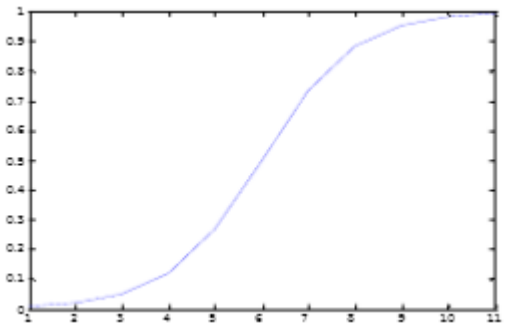 | $f(x) = \frac{1}{1 + e^{-x}}$ |

### 3.1.6 Validation of Neural Network

After the ANN model has been adequately trained, a statistical analysis will be performed to evaluate the validity of the network. The regression coefficient ($R^2$) which measures the correlation between the actual and predicted value obtained from the developed neural network will be utilized to evaluate the performance of the ANN. The closer the $R^2$ value is to 1, the higher the accuracy. The regression coefficient is calculated using Equation 3.

$$R^2 = 1 - \left[\frac{\sum_{i=1}^{N}(HWP^{exp} - HWP^{pred})^2}{\sum_{i=1}^{N}(HWP^{exp} - HWP^{mean})^2}\right] \quad (3)$$

Where:

$HWP^{exp}$: the actual experimental values of hydrogen storage capacity

$HWP^{pred}$: the model predicted values of hydrogen storage capacity

$HWP^{mean}$: the average value of the experimental data

### 3.1.7 Improvement and Use of Neural Network

If the error of validation lies outside of acceptable limits, improvement of ANN shall be made until the error falls within acceptable limits. According to the Nalbant et al. (2007), the neural network should have a prediction accuracy of above 90%. Since ANNs are data-driven models, the performance of the network can also be improved by increasing the number of data points used for the model development. However, data collection is limited by availability and accessibility of hydrogen storage data. Hence, another method which is by altering the network's architecture is applied to improve the performance of model. Until the ANN model being developed meets the level of accuracy required, its network and architecture will continuously undergo modifications. Upon, modification, the training, testing and validation are repeated in a loop until the ANN model has reached adequate accuracy.

After the ANN is trained and validated, the model can be used to calculate the network response to any input.

# CHAPTER 4

# RESULTS AND DISCUSSION

A total of 103 data points were used for the development of this ANN model. The ANN develop by using MATLAB's Neural Network Toolbox™ will predict the output which is hydrogen storage capacity (wt%) using 7 input variables: composition formula of Magnesium (Mg), Nickel (Ni), Lithium (Li), Copper (Cu), Aluminium (Al), temperature and pressure.

## 4.1 Optimization of Neural Network Architecture

3 different ANN architectures are required and constructed in the present work. These ANNs have the common training function (trainlm) and performance function which are mean square error (MSE). To acquire the best predicted output that is closed to the expected output, the architecture of the ANNs is determined in the following approach:

a) The transfer functions
b) The number of neurons in the hidden layer

### 4.1.1 Optimization of Transfer Functions in ANN

Based on Dorofki et al. (2012), the scalar input (p) is multiplied by the weight (w) and added with the bias (b). The combination is then passed to the summer. The summer output (n), also known as the net input enter the transfer function (f) to generate the scalar neuron output (a). The flow of input neuron is shown in Figure 4.1.

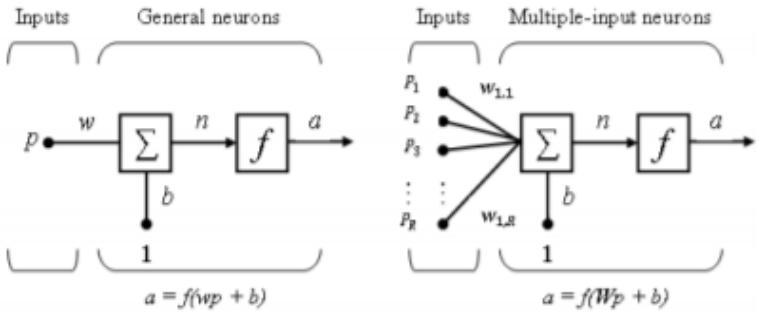


Figure 4.1: Flow of input neuron (Dorofki et al., 2012)

In this project, the MATLAB provides 3 different built-in transfer functions which are linear (purelin), Hyperbolic Tangent Sigmoid (tansig) and Logistic Sigmoid (logsig) to generate output. 3 ANNs are developed using different transfer function and trained with the same data set. The performance of the ANNs are evaluated using regression coefficient ($R^2$) which is an indication of the similarity of the model's predictions to their corresponding actual experimental values and compared in Table 4.1. The closer regression value to 1, the smaller the difference between the predicted outputs and expected output. From Table 4.1, it can be concluded that the performance of network with tansig transfer function is found good in comparison to purelin and logsig.

Table 4.1: Comparison of transfer functions

| Transfer Function | Regression Value | Overall Regression Plot |
|---|---|---|
| Purelin | 0.61796 | 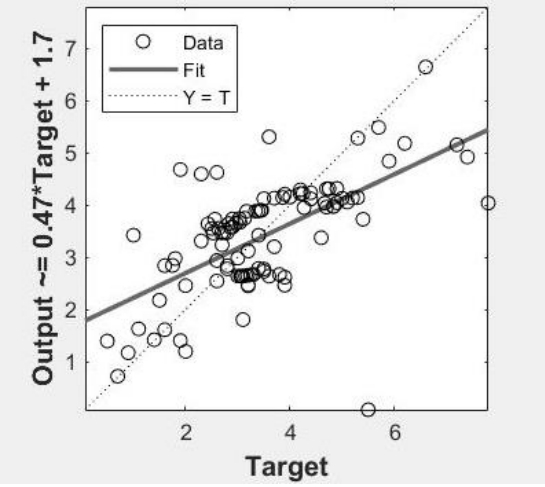 |

| | | |
|---|---|---|
| Tansig | 0.92767 | 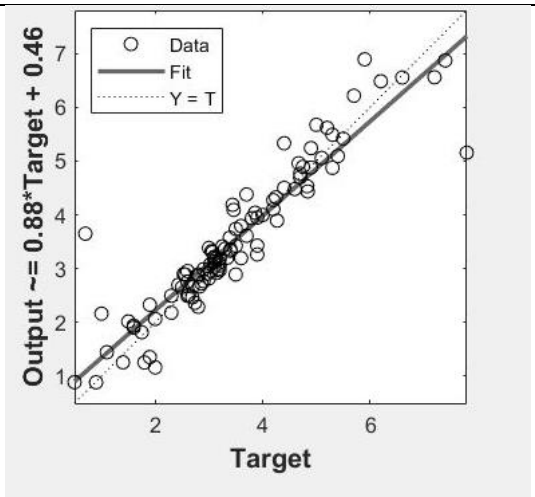 |
| Logsig | 0.88511 | 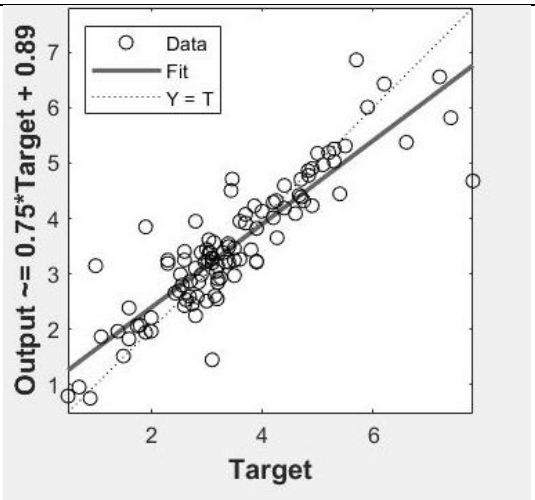 |

### 4.1.2 Optimization of Number of Neurons in ANN

The layer in the ANN model consists of a parameterizable number of neurons. Determining the number of neurons in the hidden layer is a crucial part for the overall neural network as it affects the ability of the network to separate the data (Abraham, 2005). Using a great number of hidden neurons will ensure correct learning and resulting in the network being able to predict the data accurately. However, it also causes several problems such as overfittings and compromises the performance on new data and the ability to generalize. Conversely, using too few hidden neurons in the hidden layer will lead to underfitting where the network may be unable to learn the relationships amongst the data (Abraham, 2005). Therefore, the number of hidden neurons in the hidden layer must be selected carefully.

The optimization of the number of neurons in the hidden layer is performed to determine the suitable number of hidden neurons. The number of neurons in the hidden layer is varied from 1 to 60 and the mean square error (MSE) values of each ANN model is calculated. Figure 4.2 shows the MSE of the train, validation and test sets as a function of the number of neurons in the hidden layer. From this figure, the optimum number of neurons in the hidden layer is 10 as it has the lowest MSE value for all train, validation and test sets and little to no variance between the 3 MSEs values. The MSE value closer to 0 indicate that the best performance can be obtained from the ANN with the selected number of neurons.

Besides that, it is observed that the MSE value of all data sets are higher when the number of neurons is lower (1 – 9 neurons). This denoted that ANN model with the lower number of neurons is underfitted and produce errors. On the other hand, when the number of neurons is higher than 10, the MSE values rise indicating the model is overfitted as too many neurons is presented in the ANN.

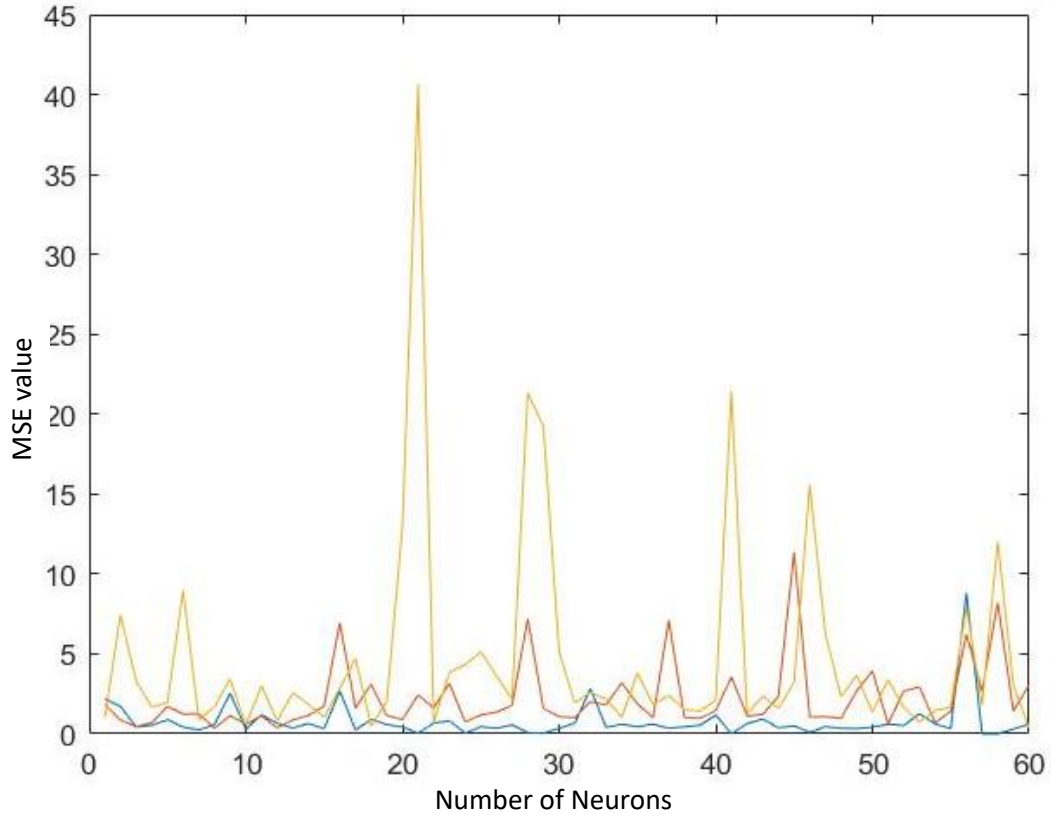


Figure 4.2: MSE values of data versus number of neurons

## 4.2 Development of Artificial Neural Network (ANN)

The ANN which is inspired by the biological neural network has 3 types of layers which are input, hidden and output. Every network has only 1 input and output layer. In the present study, the number of hidden layer is fixed as 1 as the number of datasets used is comparatively small. The developed ANN model is a feedforward ANN model as the layer feeds the input to the next layer in a feedforward manner with backpropagation algorithm. Furthermore, the training algorithm used is Levenberg-Marquardt algorithm as it is the most commonly used algorithm. From section 4.1, it is agreed that the transfer function used is Hyperbolic Tangent Sigmoid (tansig) and number of neurons in the hidden layer is 10. Figure 4.3 shown the architecture of neural network developed.

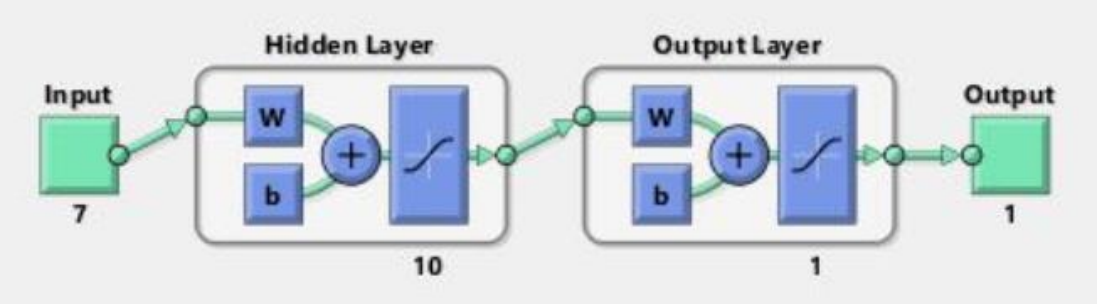


Figure 4.3: The architecture of neural network developed

## 4.3 Validation of Neural Network

The performance of the trained neural network is determined based on the accuracy of the output predicted by the model with the experimental output obtained from data collection. The statistical technique used to access the accuracy is regression coefficient ($R^2$) and it is done by fitting a set of data points to a graph. In addition to that, $R^2$ is an indication of the similarity of the model's predictions to their corresponding actual experimental values. The comparison between the predicted output and the actual output values is illustrated in Figure 4.4 together with the best fit line. The nearer the data lie to the best fit line, the higher the similarity of the ANN's predicted output and the expected output. From Figure 4.4, it can be seen that most of the data lie close to the best fit line.

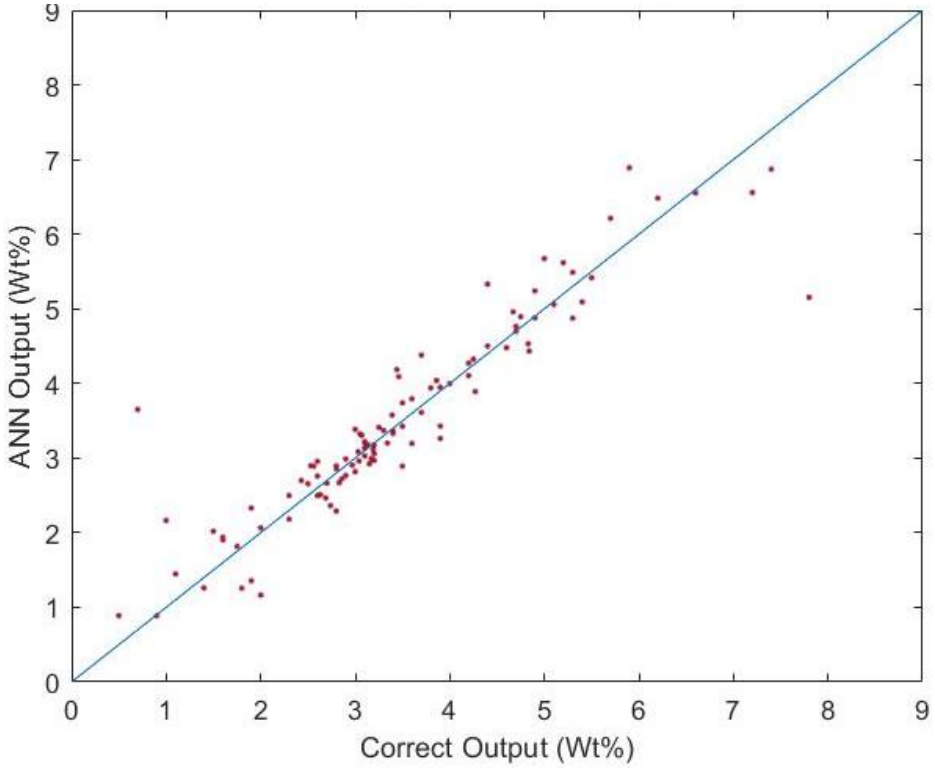


Figure 4.4: Comparison of predicted outputs and expected outputs

Further evaluation of the performance of the ANN model was performed by determining the regression values of the training, validation, test and overall sets. The regression plots and values can be obtained using Neural Network Toolbox in MATLAB after training the model. Figure 4.5 shown the regression plot and values of training, validation, test and overall sets. From Figure 4.5, the regression values for the training, validation, and testing sets are 0.9076, 0.97631 and 0.97098 respectively, resulting in an overall regression value of 0.92767. All data sets have regression values higher than 0.90. Hence, it can be concluded that the model is able to generate predictions with over 90% accuracy.

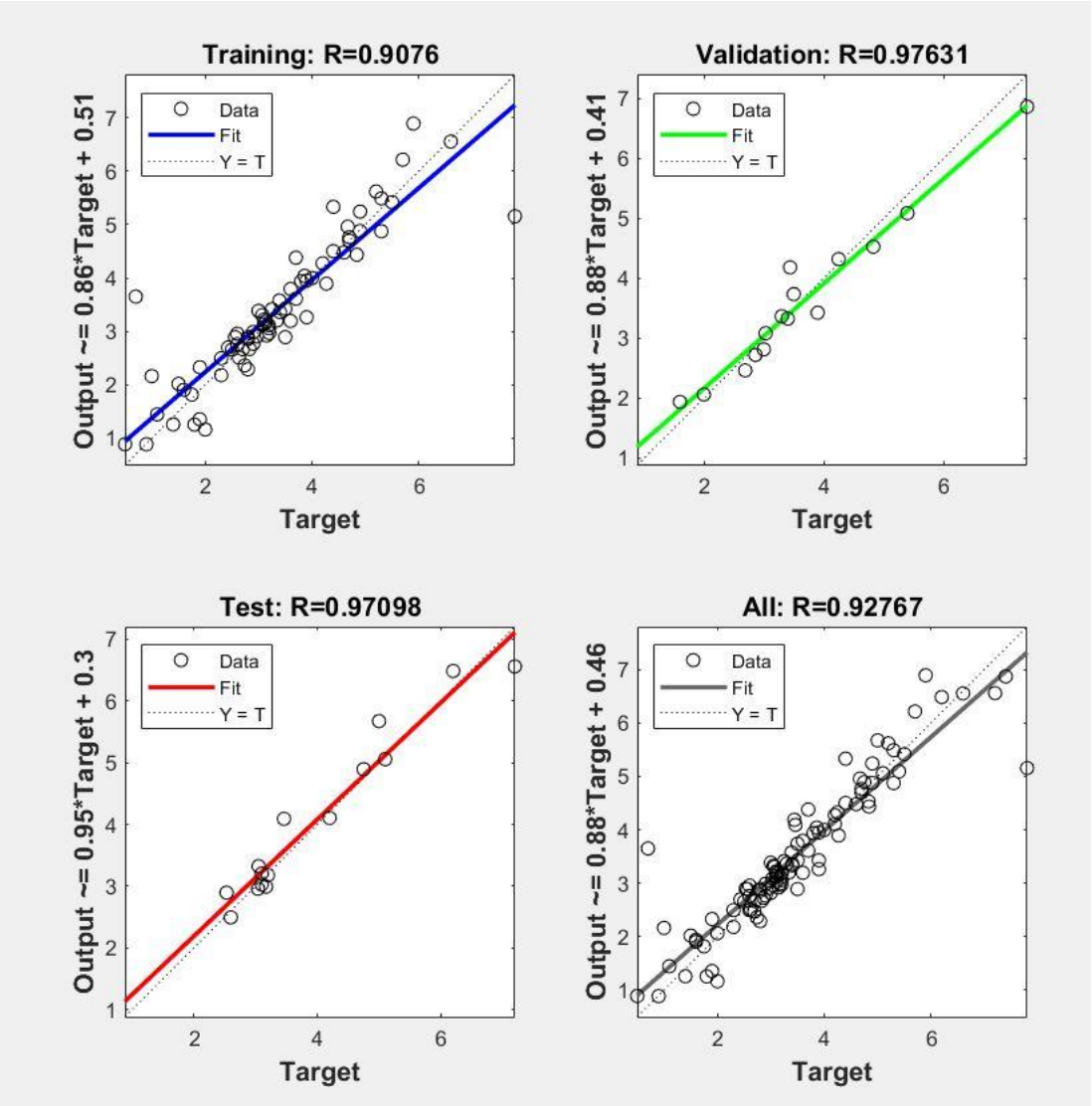


Figure 4.5: Regression plots and values of ANN

## 4.4 Analysis of Inputs

Based on the results obtained in section 4.3, the developed ANN model is able to predict the hydrogen storage capacity of the Mg based hydrides using the inputs: composition of Magnesium (Mg), Nickel (Ni), Lithium (Li), Copper (Cu), Aluminium (Al), temperature and pressure. In order to understand the importance of each alloy materials on the predicted values, the ANN developed was used to examine the influence of varying the composition input while fixing the remaining parameters. In this study, the temperature and pressure are assumed to be 300℃ and 10 bar. Figure 4.6 shows the effect of hydrogen storage capacity when the composition of Mg hydrides is varied from 0 to 1.

As shown in Figure 4.6, when the composition of Mg in the hydride is 0, it denotes that there is only Ni, Cu and Al present and their hydrogen storage capacity are 1.56wt%, 1.3wt% and 4.9wt% respectively. Conversely, when the composition of Mg in the hydride is 1, meaning that only Mg present in the system, it has the highest hydrogen storage capacity of 5.93wt%. However, pure Mg is not a suitable hydrogen storage material as it has many drawbacks such as the poor kinetics of the hydrogen charging/ decharging cycle (Bahou et al., 2020; Peng et al., 2017; Zhang et al., 2017; Čermák et al., 2008).

Based on Figure 4.6, the most promising hydrogen storage capacity result is obtained by alloying Mg with Ni as it has the second hydrogen storage capacity which is 5.91wt% when composition of Mg is 0.9 and Ni is 0.1. The reduce in hydrogen storage capacity is due to the addition of Ni for the purpose of lowering the formation enthalpy. According to Muthukumar et al. (2008), the $Mg_2Ni$ only have 3.4wt% of hydrogen whereas the predicted hydrogen storage capacity generated when $Mg_2Ni$ is 3.1wt%, having very small error of 8.82% which is shown in Table 4.2. This small error proved the ability of ANN to predict accurate results.

In addition to that, a similar trend is expected for the alloy of Cu in Mg where the hydrogen capacity will decrease with the increase of composition of Cu. In Figure 4.6, a decreasing trend in hydrogen storage capacity is observed as the composition of

Cu is increased, thus confirming the expected trend. This trend is further supported by Crivello et al. (2016) as the reduction in particle size for the sorption kinetics is at the expense of hydrogen storage capacity. The same trend goes to $Mg_XAl_{1-X}$. when composition of Mg is from 0.78 to 1, the hydrogen storage capacity started to fluctuate before 0.78 composition of Mg.

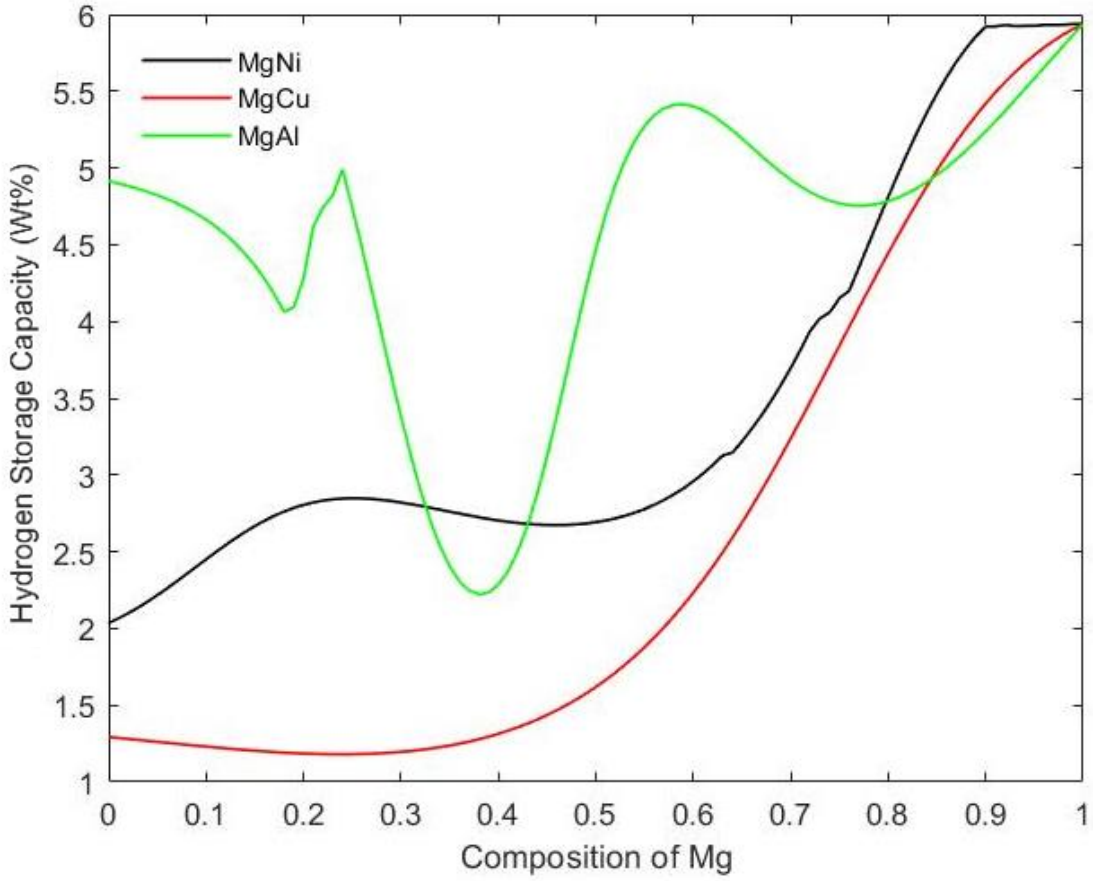


Figure 4.6: Graph of hydrogen storage capacity (wt%) with varying composition of Mg, Ni, Li, Cu, Al

Table 4.2: Comparison between the actual value and predicted value

| Formula | Actual Value (wt%) | Predicted Value (wt%) | Error (%) |
|---|---|---|---|
| $Mg_2Ni$ | 3.4 (Muthukumar et al.,2008) | 3.1 | 8.82 |
| MgAl | 4.6 (Wang et al., 2017) | 4.47 | 2.83 |

As the $Mg_{0.9}Ni_{0.1}$ is discovered as the promising hydrogen storage material, the addition of a third component such as another transition metal (Cu) can further improve the hydrogenation kinetics of the storage systems and making it a better choice for hydrogen storage (Milanese et al., 2010). Hence, the effect on hydrogen storage capacity with the addition of Cu and Li in MgNi is investigated and shown in Figure 4.7. From Figure 4.7, the hydrogen storage capacity decrease as the composition of the third component increase. The experiment research conducted by Milanese et al. (2010) had supported the trend as a rise in 10wt% of Cu in MgNi caused the maximum hydrogen capacity to be reduced by 1wt%. On top of that, the decrease in hydrogen capacity with increasing Li content is proven by Wu et al. (2019).

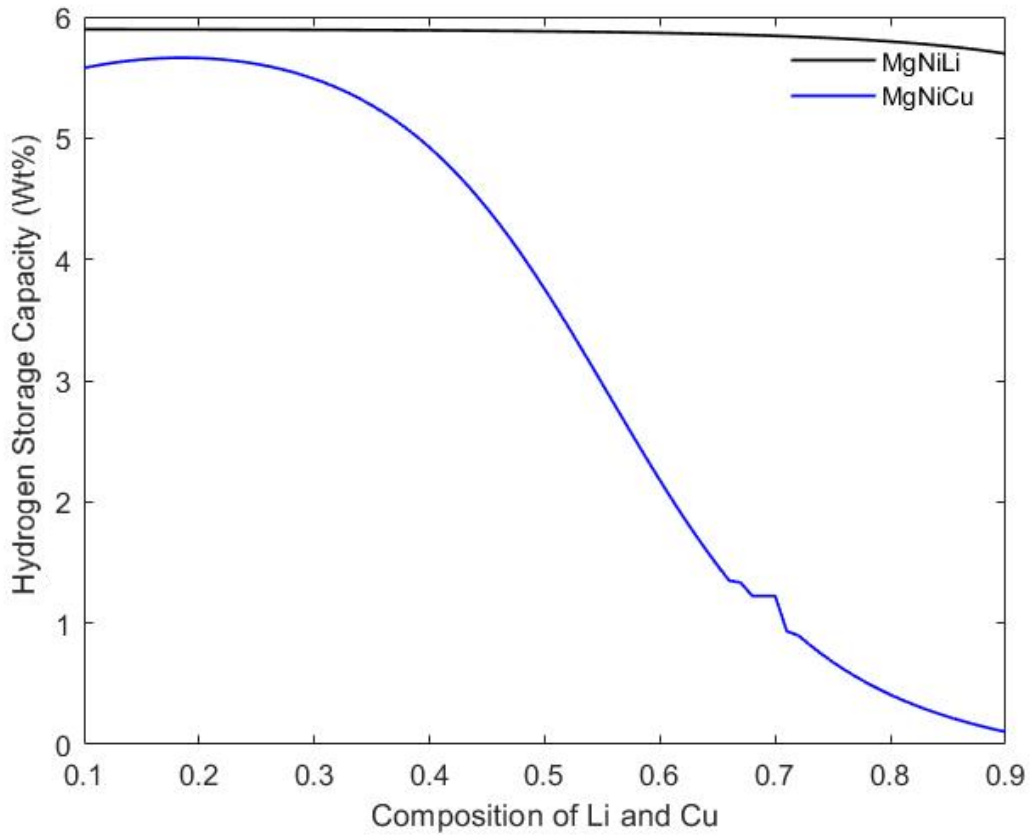


Figure 4.7: Graph of hydrogen storage capacity (wt%) with varying composition of Li and Cu in MgNi

Through varying the composition of alloy materials in Mg hydride, it can be concluded that increasing the composition of alloy material led to a lower hydrogen storage capacity.

Apart from evaluation of the effect of the material composition on predicted hydrogen storage capacity, the influence of pressure and temperature on the predicted hydrogen storage capacity is performed by fixing the remaining parameters such as composition of Magnesium (Mg), Nickel (Ni), Lithium (Li), Copper (Cu) and Aluminium (Al). Figure 4.8 and 4.9 illustrate the effect of varying pressure and temperature on the hydrogen storage capacity of $Mg_{0.667}Ni_{0.333}$. The ranges of pressure and temperature utilized for the development of the ANN model is 0.004 bar to 57 bar and 25℃ to 450℃ respectively. In order to ensure that the ANN model is able to make highly accurate predictions, the odd data is neglected. Hence, the ranges of pressure and temperature used to access their influence on the predicted hydrogen hydrogen storage capacity is 10 bar to 40 bar and 300℃ to 400℃.

The expected trend for hydrogen storage in Mg based hydrides with respect to pressure is that increasing pressure would result in greater hydrogen storage capacity. Figure 4.8 shows that the hydrogen storage capacity increase with the rise of pressure, thus the expected trend is verified.

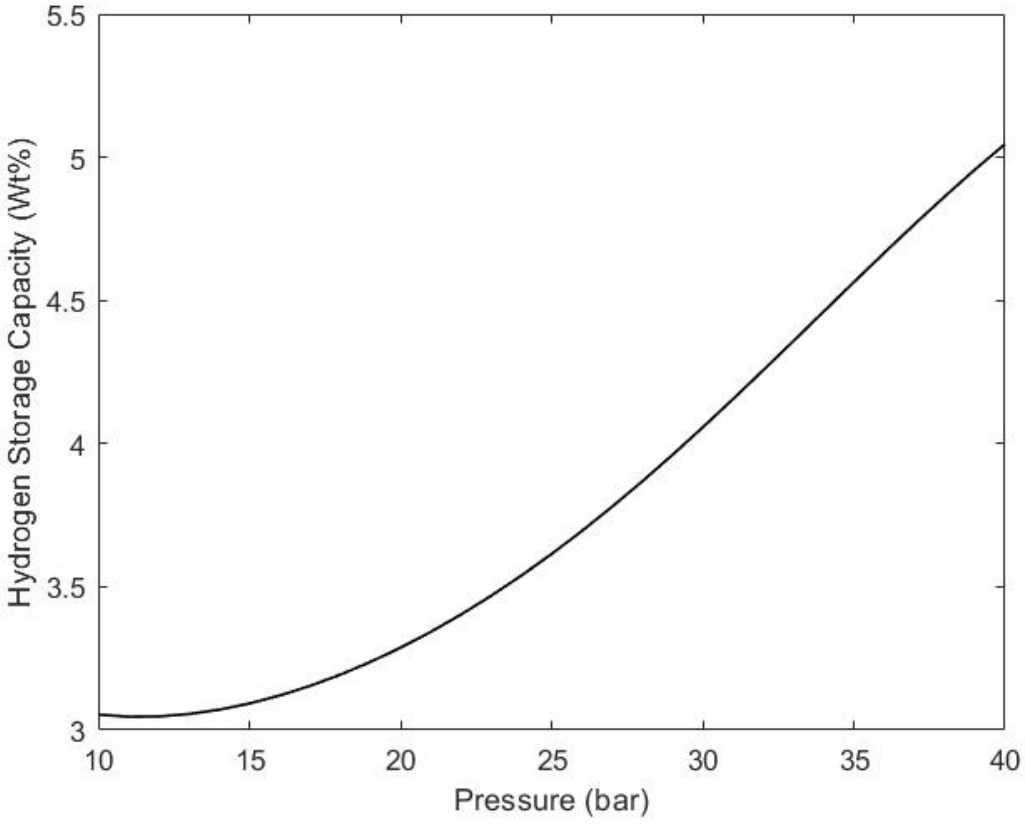


Figure 4.8: Graph of hydrogen storage capacity (wt%) with varying pressure

The expected trend for hydrogen storage capacity in Mg based hydrides with respect to temperature is that increasing temperature would result in a higher hydrogen storage capacity. Figure 4.9 shows that the hydrogen storage capacity increase with the rise of temperature, thus the expected trend is verified.

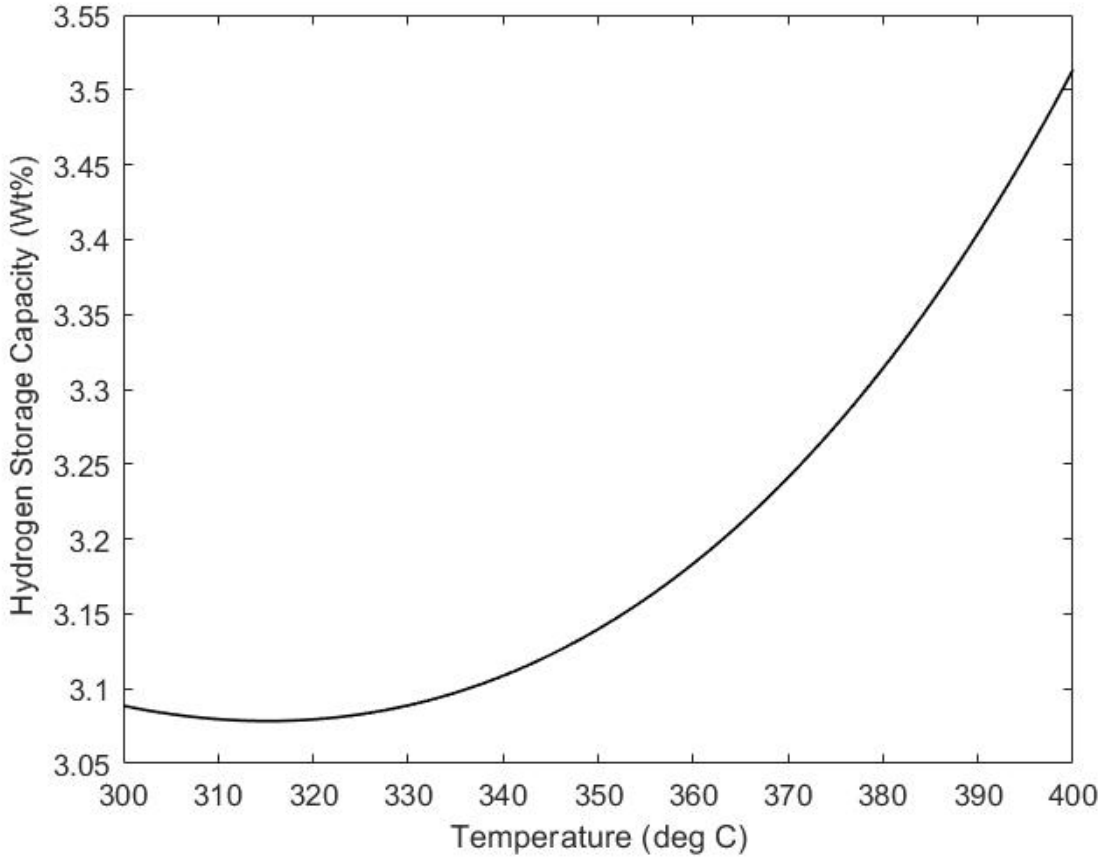


Figure 4.9: Graph of hydrogen storage capacity (wt%) with varying temperature

In summation, the results show that hydrogen storage capacity is depended on the parameters selected which are composition of Magnesium (Mg), Nickel (Ni), Lithium (Li), Copper (Cu), Aluminium (Al), temperature and pressure. Besides that, it is justified that ANN is a feasible tool for the prediction of hydrogen storage capacity of Mg based hydrides as the ANN developed is capable of generating accurate predictions of hydrogen storage capacity when the input parameters varied.

# CHAPTER 5

# CONCLUSION AND RECOMMENDATION

## 5.1 Conclusion

An ANN model has been created for the prediction of the hydrogen storage capacity of Mg based alloy hydrides as a function of the alloy composition, pressure and temperature. The input parameters are the composition of Magnesium (Mg), Nickel (Ni), Lithium (Li), Copper (Cu), Aluminium (Al), temperature and pressure while the output parameter is hydrogen storage capacity. In the present study, a total of 103 data were used to develop the ANN model. The architecture of the model consists of one hidden layer with 10 neurons as it was found to have the lowest MSE and utilized tansig transfer function which has a higher regression value compared to other built-in transfer function. The regression analysis conducted showed that the developed model is able to predict accurate hydrogen storage capacity which is indicated by its overall regression coefficient of 0.92767.

Besides that, the developed model is used to study the influence of the alloying elements, temperature and pressure on the hydrogen storage capacity. Increasing of the composition of alloying material results in a decrease in hydrogen storage capacity with the exception for Al in Mg as it fluctuated before Mg composition is 0.78. On the other hand, the hydrogen storage capacity rises with the increase of pressure and temperature. The results of this study prove that the ANN is a feasible tool for modelling the prediction of hydrogen storage capacity in Magnesium alloy hydrides at different temperature and pressure.

## 5.2 Recommendation

One of the limitations encountered in this study is the lack of availability of data points from the literature. This might limit the capability of ANN model to predict more accurate and reliable outcome as ANN is a data driven model. Therefore, the improvement of this developed ANN model can be made by increasing the number of data used.

## REFERENCES


Abe, J. O., Popoola, A. P. I., Ajenifuja, E., & Popoola, O. M. (2019). Hydrogen energy, economy and storage: Review and recommendation. In *International Journal of Hydrogen Energy* (Vol. 44, Issue 29, pp. 15072–15086). Elsevier Ltd. https://doi.org/10.1016/j.ijhydene.2019.04.068

Abraham, A. (2005). Artificial Neural Networks. In *Handbook of Measuring System Design*. John Wiley & Sons, Ltd. https://doi.org/10.1002/0471497398.mm421

Al Shamisi, M. H., H., A., & N. Hejase, H. A. (2011). Using MATLAB to Develop Artificial Neural Network Models for Predicting Global Solar Radiation in Al Ain City – UAE. In *Engineering Education and Research Using MATLAB*. InTech. https://doi.org/10.5772/25213

Andersson, J., & Grönkvist, S. (2019). Large-scale storage of hydrogen. In *International Journal of Hydrogen Energy* (Vol. 44, Issue 23, pp. 11901–11919). Elsevier Ltd. https://doi.org/10.1016/j.ijhydene.2019.03.063

Anghel, D. C., Ene, A., & Belu, N. (2014). A matlab neural network application for the study of working conditions. *Advanced Materials Research*, *837*, 310–315. https://doi.org/10.4028/www.scientific.net/AMR.837.310

AZoCleantech. (2008). *Hydrogen Energy - The Perfect Energy Source for the Future?* https://www.azocleantech.com/article.aspx?ArticleID=29

Bahou, S., Labrim, H., Lakhal, M., Bhihi, M., Hartiti, B., & Ez-Zahraouy, H. (2020). Magnesium vacancies and hydrogen doping in MgH2 for improving gravimetric capacity and desorption temperature. *International Journal of Hydrogen Energy*. https://doi.org/10.1016/j.ijhydene.2020.10.078

Barthelemy, H., Weber, M., & Barbier, F. (2017). Hydrogen storage: Recent improvements and industrial perspectives. *International Journal of Hydrogen Energy*, *42*(11), 7254–7262. https://doi.org/10.1016/j.ijhydene.2016.03.178

Bellosta von Colbe, J., Ares, J. R., Barale, J., Baricco, M., Buckley, C., Capurso, G., Gallandat, N., Grant, D. M., Guzik, M. N., Jacob, I., Jensen, E. H., Jensen, T., Jepsen, J., Klassen, T., Lototskyy, M. V., Manickam, K., Montone, A., Puszkiel, J., Sartori, S., … Dornheim, M. (2019). Application of hydrides in hydrogen storage and compression: Achievements, outlook and perspectives. *International Journal of Hydrogen Energy*, *44*(15), 7780–7808. https://doi.org/10.1016/j.ijhydene.2019.01.104

Breeze, P. (2018). Hydrogen Energy Storage. In *Power System Energy Storage Technologies* (pp. 69–77). Elsevier. https://doi.org/10.1016/b978-0-12-812902-9.00008-0

Brownlee, J. (2016). *How to Code a Neural Network with Backpropagation In Python (from scratch)*. https://machinelearningmastery.com/implement-backpropagation-algorithm-scratch-python/

Čermák, J., Král, L., & David, B. (2008). Hydrogen diffusion in Mg2NiH4 intermetallic compound. *Intermetallics*, *16*(4), 508–517. https://doi.org/10.1016/j.intermet.2007.12.010

Chamoun, R., Demirci, U. B., & Miele, P. (2015). Cyclic Dehydrogenation-(Re)Hydrogenation with Hydrogen-Storage Materials: An Overview. *Energy Technology*, *3*(2), 100–117. https://doi.org/10.1002/ente.201402136

Crivello, J. C., Denys, R. V., Dornheim, M., Felderhoff, M., Grant, D. M., Huot, J., Jensen, T. R., de Jongh, P., Latroche, M., Walker, G. S., Webb, C. J., & Yartys, V. A. (2016). Mg-based compounds for hydrogen and energy storage. *Applied Physics A: Materials Science and Processing*, *122*(2), 1–17. https://doi.org/10.1007/s00339-016-9601-1

Dornheim, M. (2011). Thermodynamics of Metal Hydrides: Tailoring Reaction Enthalpies of Hydrogen Storage Materials. In *Thermodynamics - Interaction Studies - Solids, Liquids and Gases*. InTech. https://doi.org/10.5772/21662

Dorofki, M., Elshafie, A. H., Jaafar, O., Karim, O. A., & Mastura, S. (2012). *Comparison of Artificial Neural Network Transfer Functions Abilities to Simulate Extreme Runoff Data*.

*Energy – United Nations Sustainable Development*. (n.d.). Retrieved November 9, 2020, from https://www.un.org/sustainabledevelopment/energy/

Hua, T. Q., Ahluwalia, R. K., Peng, J. K., Kromer, M., Lasher, S., McKenney, K., Law, K., & Sinha, J. (2011). Technical assessment of compressed hydrogen storage tank systems for automotive applications. *International Journal of Hydrogen Energy*, *36*(4), 3037–3049. https://doi.org/10.1016/j.ijhydene.2010.11.090

Jain, I. P. (2009). Hydrogen the fuel for 21st century. *International Journal of Hydrogen Energy*, *34*(17), 7368–7378. https://doi.org/10.1016/j.ijhydene.2009.05.093

Ji, L., Zhang, L., Yang, X., Zhu, X., & Chen, L. (2020). The remarkably improved hydrogen storage performance of MgH2 by the synergetic effect of an FeNi/rGO nanocomposite. *Dalton Transactions*, *49*(13), 4146–4154. https://doi.org/10.1039/d0dt00230e

Krishna, R., Titus, E., Salimian, M., Okhay, O., Rajendran, S., Rajkumar, A., G. Sousa, J. M., C. Ferreira, A. L., Campos, J., & Gracio, J. (2012). Hydrogen Storage for Energy Application. In *Hydrogen Storage*. InTech. https://doi.org/10.5772/51238

Lenahan, M. (2011). Hydrogen Storage Materials Database Demonstration. *Journal of the Society of Materials Science, Japan*. http://www.hydrogenmaterialssearch.govtools.us/

Liu, H. (2010). On the Levenberg-Marquardt training method for feed-forward neural networks. *Proceedings - 2010 6th International Conference on Natural Computation, ICNC 2010*, *1*, 456–460. https://doi.org/10.1109/ICNC.2010.5583151

Malinova, T., & Guo, Z. X. (2004). Artificial neural network modelling of hydrogen storage properties of Mg-based alloys. *Materials Science and Engineering A*, *365*(1–2), 219–227. https://doi.org/10.1016/j.msea.2003.09.031

Milanese, C., Girella, A., Bruni, G., Berbenni, V., Cofrancesco, P., Marini, A., Villa, M., & Matteazzi, P. (2008). Hydrogen storage in magnesium-metal mixtures: Reversibility, kinetic aspects and phase analysis. *Journal of Alloys and Compounds*, *465*(1–2), 396–405. https://doi.org/10.1016/j.jallcom.2007.10.091

Milanese, C., Girella, A., Bruni, G., Cofrancesco, P., Berbenni, V., Matteazzi, P., & Marini, A. (2010). Mg-Ni-Cu mixtures for hydrogen storage: A kinetic study. *Intermetallics*, *18*(2), 203–211. https://doi.org/10.1016/j.intermet.2009.07.012

Montone, A., Aurora, A., Mirabile Gattia, D., & Vittori Antisari, M. (2011). Effect of hydrogen pressure and temperature on the reaction kinetics between Fe-doped Mg and hydrogen gas. *Journal of Alloys and Compounds*, *509*(SUPPL. 2), S580–S583. https://doi.org/10.1016/j.jallcom.2010.10.096

Muthukumar, P., Maiya, M. P., Srinivasa Murthy, S., Vijay, R., & Sundaresan, R. (2008). Tests on mechanically alloyed Mg2Ni for hydrogen storage. *Journal of Alloys and Compounds*, *452*(2), 456–461. https://doi.org/10.1016/j.jallcom.2007.03.112

Nalbant, M., Gokkaya, H., Ihsan, ˙, & Toktas¸, T. (2007). *Comparison of Regression and Artificial Neural Network Models for Surface Roughness Prediction with the Cutting Parameters in CNC Turning*. 14. https://doi.org/10.1155/2007/92717

Peng, X., Wang, H., Hu, R., Ouyang, L., Liu, J., & Zhu, M. (2017). Electrochemical performances of MgH2 and MgH2-C films for lithium ion battery anode. *Journal of Alloys and Compounds*, *711*, 473–479. https://doi.org/10.1016/j.jallcom.2017.03.180

Rabienataj Darzi, A. A., Hassanzadeh Afrouzi, H., Moshfegh, A., & Farhadi, M. (2016). Absorption and desorption of hydrogen in long metal hydride tank equipped with phase change material jacket. *International Journal of Hydrogen Energy*, *41*(22), 9595–9610. https://doi.org/10.1016/j.ijhydene.2016.04.051

Rapier, R. (2020). *Fossil Fuels Still Supply 84 Percent Of World Energy — And Other Eye Openers From BP's Annual Review*. https://www.forbes.com/sites/rrapier/2020/06/20/bp-review-new-highs-in-global-energy-consumption-and-carbon-emissions-in-2019/?sh=7df062b066a1

Sakintuna, B., Lamari-Darkrim, F., & Hirscher, M. (2007). Metal hydride materials for solid hydrogen storage: A review. In *International Journal of Hydrogen Energy* (Vol. 32, Issue 9, pp. 1121–1140). Pergamon. https://doi.org/10.1016/j.ijhydene.2006.11.022

Sasaki, K., Li, H.-W., Hayashi, A., Yamabe, J., & Ogura, T. (2016). Hydrogen Energy Engineering. In K. Sasaki, H.-W. Li, A. Hayashi, J. Yamabe, T. Ogura, & S. M. Lyth (Eds.), *Hydrogen Energy Engineering*. Springer Japan. https://doi.org/10.1007/978-4-431-56042-5

*Solutions to the energy crisis: how to achieve sustainable energy?* (n.d.). Retrieved November 9, 2020, from https://solarimpulse.com/energy-crisis-solutions

Sun, Z., Lu, X., Nyahuma, F. M., Yan, N., Xiao, J., Su, S., & Zhang, L. (2020). Enhancing Hydrogen Storage Properties of MgH2 by Transition Metals and Carbon Materials: A Brief Review. In *Frontiers in Chemistry* (Vol. 8, p. 552). Frontiers Media S.A. https://doi.org/10.3389/fchem.2020.00552

Wang, Y., Lü, S., Zhou, Z., Zhou, W., Guo, J., & Lan, Z. (2017). Effect of transition metal on the hydrogen storage properties of Mg–Al alloy. *Journal of Materials Science*, *52*(5), 2392–2399. https://doi.org/10.1007/s10853-016-0533-0

Webb, C. J. (2015). A review of catalyst-enhanced magnesium hydride as a hydrogen storage material. *Journal of Physics and Chemistry of Solids*, *84*(1), 96–106. https://doi.org/10.1016/j.jpcs.2014.06.014

Wu, C. T., Liu, J. H., & Tsai, T. H. (2019). Effects of volatilization of lithium on hydrogen storage characteristics of Mg-Ni-Li alloy. *Journal of Materials Research*, *34*(20), 3583–3588. https://doi.org/10.1557/jmr.2019.287

Yanxing, Z., Maoqiong, G., Yuan, Z., Xueqiang, D., & Jun, S. (2019). Thermodynamics analysis of hydrogen storage based on compressed gaseous hydrogen, liquid hydrogen and cryo-compressed hydrogen. *International Journal of Hydrogen Energy*, *44*(31), 16833–16840. https://doi.org/10.1016/j.ijhydene.2019.04.207

Yartys, V. A., Lototskyy, M. V., Akiba, E., Albert, R., Antonov, V. E., Ares, J. R., Baricco, M., Bourgeois, N., Buckley, C. E., Bellosta von Colbe, J. M., Crivello, J. C., Cuevas, F., Denys, R. V., Dornheim, M., Felderhoff, M., Grant, D. M., Hauback, B. C., Humphries, T. D., Jacob, I., … Zhu, M. (2019). Magnesium based materials for hydrogen based energy storage: Past, present and future. *International Journal of Hydrogen Energy*, *44*(15), 7809–7859. https://doi.org/10.1016/j.ijhydene.2018.12.212

Zhang, Y., Zhang, W., Yuan, Z., Bu, W., Qi, Y., & Guo, S. (2017). Improvement on hydrogen storage thermodynamics and kinetics of the as-milled SmMg11Ni alloy by adding MoS2. *International Journal of Hydrogen Energy*, *42*(27), 17157–17166. https://doi.org/10.1016/j.ijhydene.2017.05.179

# APPENDICES

## APPENDIX A: Experimental data for model development

| Item No. | Composition Formula | | | | | Temperature (°C) | Pressure (Atmospheres Absolute) bar | Hydrogen Storage Capacity (wt%) |
|---|---|---|---|---|---|---|---|---|
| | Mg | Ni | Li | Cu | Al | | | |
| 1 | 0.037 | 0 | 0 | 0.963 | 0 | 330 | 3.2 | 5.3 |
| 2 | 0.0385 | 0.9615 | 0 | 0 | 0 | 323 | 3 | 5.7 |
| 3 | 0.045 | 0 | 0 | 0 | 0.955 | 352 | 6 | 6.6 |
| 4 | 0.09 | 0.91 | 0 | 0 | 0 | 292 | 1.3 | 7.2 |
| 5 | 0.09 | 0.91 | 0 | 0 | 0 | 300 | 2 | 6.2 |
| 6 | 0.09 | 0.91 | 0 | 0 | 0 | 335 | 9 | 3.6 |
| 7 | 0.167 | 0.833 | 0 | 0 | 0 | 300 | 1.4 | 5.9 |
| 8 | 0.167 | 0.833 | 0 | 0 | 0 | 323 | 2.9 | 7.4 |
| 9 | 0.333 | 0.333 | 0 | 0 | 0.333 | 300 | 8 | 3.5 |
| 10 | 0.333 | 0.333 | 0 | 0 | 0.333 | 300 | 17 | 3.7 |
| 11 | 0.333 | 0.333 | 0 | 0 | 0.333 | 300 | 35 | 4 |
| 12 | 0.333 | 0.333 | 0 | 0 | 0.333 | 300 | 27 | 3.86 |
| 13 | 0.333 | 0.333 | 0 | 0 | 0.333 | 325 | 24 | 4.25 |
| 14 | 0.333 | 0.333 | 0 | 0 | 0.333 | 325 | 20 | 4.2 |
| 15 | 0.333 | 0.333 | 0 | 0 | 0.333 | 325 | 10 | 3.9 |
| 16 | 0.333 | 0.333 | 0 | 0 | 0.333 | 325 | 34 | 4.4 |
| 17 | 0.333 | 0.333 | 0 | 0 | 0.333 | 350 | 34 | 4.9 |
| 18 | 0.333 | 0.333 | 0 | 0 | 0.333 | 350 | 10 | 4.2 |
| 19 | 0.333 | 0.333 | 0 | 0 | 0.333 | 350 | 30 | 4.75 |
| 20 | 0.333 | 0.333 | 0 | 0 | 0.333 | 350 | 26 | 4.7 |
| 21 | 0.4 | 0 | 0 | 0 | 0.6 | 326 | 10 | 2.3 |
| 22 | 0.4 | 0 | 0 | 0 | 0.6 | 335 | 11 | 2.6 |
| 23 | 0.4 | 0 | 0 | 0 | 0.6 | 350 | 14 | 1.9 |
| 24 | 0.5 | 0 | 0 | 0 | 0.5 | 280 | 5 | 3.34 |
| 25 | 0.5 | 0 | 0 | 0 | 0.5 | 280 | 7 | 3.39 |
| 26 | 0.5 | 0 | 0 | 0 | 0.5 | 280 | 22 | 3.46 |
| 27 | 0.5 | 0 | 0 | 0 | 0.5 | 280 | 16 | 3.44 |
| 28 | 0.5 | 0 | 0 | 0 | 0.5 | 280 | 4 | 3.17 |
| 29 | 0.5 | 0.5 | 0 | 0 | 0 | 25 | 0.004 | 2 |
| 30 | 0.5 | 0.5 | 0 | 0 | 0 | 140 | 0.7 | 1.6 |
| 31 | 0.5 | 0.5 | 0 | 0 | 0 | 140 | 3 | 1.75 |
| 32 | 0.5 | 0.5 | 0 | 0 | 0 | 300 | 1.1 | 4.6 |
| 33 | 0.5 | 0 | 0 | 0 | 0.5 | 300 | 6 | 4.27 |
| 34 | 0.5 | 0 | 0 | 0 | 0.5 | 300 | 25.9 | 4.83 |
| 35 | 0.5 | 0 | 0 | 0 | 0.5 | 300 | 30 | 4.84 |
| 36 | 0.5 | 0 | 0 | 0 | 0.5 | 300 | 16 | 4.7 |
| 37 | 0.5 | 0.5 | 0 | 0 | 0 | 325 | 9.3 | 2.69 |
| 38 | 0.5 | 0.5 | 0 | 0 | 0 | 325 | 6.7 | 2.53 |
| 39 | 0.5 | 0.5 | 0 | 0 | 0 | 325 | 10.6 | 2.74 |
| 40 | 0.5 | 0.5 | 0 | 0 | 0 | 325 | 14 | 2.8 |
| 41 | 0.5 | 0 | 0 | 0 | 0.5 | 325 | 9.38 | 4.67 |
| 42 | 0.5 | 0 | 0 | 0 | 0.5 | 325 | 12 | 4.8 |
| 43 | 0.5 | 0 | 0 | 0 | 0.5 | 325 | 15.5 | 4.9 |

| | | | | | | | | |
|---|---|---|---|---|---|---|---|---|
| 44 | 0.5 | 0 | 0 | 0 | 0.5 | 325 | 28 | 5.1 |
| 45 | 0.5 | 0.5 | 0 | 0 | 0 | 350 | 36 | 2.9 |
| 46 | 0.5 | 0.5 | 0 | 0 | 0 | 350 | 27.7 | 2.86 |
| 47 | 0.5 | 0.5 | 0 | 0 | 0 | 350 | 12.3 | 2.63 |
| 48 | 0.5 | 0.5 | 0 | 0 | 0 | 350 | 10.5 | 2.5 |
| 49 | 0.5 | 0 | 0 | 0 | 0.5 | 350 | 23.3 | 5.2 |
| 50 | 0.5 | 0 | 0 | 0 | 0.5 | 350 | 8.7 | 4.4 |
| 51 | 0.5 | 0 | 0 | 0 | 0.5 | 350 | 18.3 | 5 |
| 52 | 0.5 | 0 | 0 | 0 | 0.5 | 350 | 30 | 5.3 |
| 53 | 0.5 | 0.5 | 0 | 0 | 0 | 375 | 40.16 | 3.04 |
| 54 | 0.5 | 0.5 | 0 | 0 | 0 | 375 | 31.1 | 2.97 |
| 55 | 0.5 | 0.5 | 0 | 0 | 0 | 375 | 19.5 | 2.83 |
| 56 | 0.5 | 0.5 | 0 | 0 | 0 | 375 | 14 | 2.43 |
| 57 | 0.5 | 0.5 | 0 | 0 | 0 | 400 | 36.3 | 3.13 |
| 58 | 0.5 | 0.5 | 0 | 0 | 0 | 400 | 29.3 | 3.03 |
| 59 | 0.5 | 0.5 | 0 | 0 | 0 | 400 | 24.74 | 2.9 |
| 60 | 0.5 | 0.5 | 0 | 0 | 0 | 400 | 20 | 2.56 |
| 61 | 0.556 | 0 | 0 | 0 | 0.444 | 326 | 7 | 5.4 |
| 62 | 0.567 | 0.333 | 0 | 0 | 0.1 | 312 | 4.5 | 2.7 |
| 63 | 0.59 | 0 | 0.05 | 0 | 0.36 | 310 | 0.7 | 1.8 |
| 64 | 0.59 | 0.05 | 0 | 0 | 0.36 | 310 | 1.8 | 3.4 |
| 65 | 0.593 | 0 | 0 | 0.296 | 0.111 | 330 | 3 | 3.2 |
| 66 | 0.6 | 0 | 0 | 0 | 0.4 | 310 | 0.7 | 1 |
| 67 | 0.6 | 0.4 | 0 | 0 | 0 | 300 | 3.7 | 2.6 |
| 68 | 0.61 | 0 | 0.085 | 0 | 0.305 | 352 | 15 | 3.8 |
| 69 | 0.615 | 0 | 0 | 0.308 | 0.077 | 330 | 3 | 3 |
| 70 | 0.62 | 0 | 0 | 0 | 0.38 | 310 | 1.4 | 2.3 |
| 71 | 0.636 | 0.364 | 0 | 0 | 0 | 300 | 4.5 | 2.8 |
| 72 | 0.64 | 0.333 | 0 | 0 | 0.027 | 295 | 4 | 3.5 |
| 73 | 0.64 | 0 | 0 | 0.32 | 0.04 | 330 | 11 | 2.8 |
| 74 | 0.667 | 0.333 | 0 | 0 | 0 | 250 | 1.1 | 3.2 |
| 75 | 0.667 | 0.25 | 0 | 0.083 | 0 | 250 | 1.2 | 3.2 |
| 76 | 0.667 | 0 | 0 | 0.333 | 0 | 295 | 6 | 2.6 |
| 77 | 0.667 | 0.333 | 0 | 0 | 0 | 299 | 3.2 | 3.6 |
| 78 | 0.667 | 0.333 | 0 | 0 | 0 | 300 | 3.7 | 3.1 |
| 79 | 0.667 | 0.333 | 0 | 0 | 0 | 300 | 2.2 | 3 |
| 80 | 0.667 | 0.333 | 0 | 0 | 0 | 300 | 3.2 | 3.1 |
| 81 | 0.667 | 0.333 | 0 | 0 | 0 | 300 | 3.1 | 3.1 |
| 82 | 0.667 | 0.333 | 0 | 0 | 0 | 300 | 2.5 | 3.05 |
| 83 | 0.667 | 0.333 | 0 | 0 | 0 | 300 | 2.6 | 3.07 |
| 84 | 0.667 | 0.333 | 0 | 0 | 0 | 300 | 10.38 | 3.15 |
| 85 | 0.667 | 0.333 | 0 | 0 | 0 | 300 | 14.7 | 3.19 |
| 86 | 0.667 | 0.333 | 0 | 0 | 0 | 300 | 23.3 | 3.5 |
| 87 | 0.667 | 0.333 | 0 | 0 | 0 | 300 | 30 | 3.9 |
| 88 | 0.667 | 0.283 | 0 | 0 | 0.05 | 327 | 3 | 3.4 |
| 89 | 0.667 | 0.333 | 0 | 0 | 0 | 450 | 57 | 3.7 |
| 90 | 0.69 | 0.31 | 0 | 0 | 0 | 323 | 4.9 | 3.9 |
| 91 | 0.7 | 0.1 | 0.1 | 0.1 | 0 | 310 | 1 | 1.6 |
| 92 | 0.7 | 0 | 0.2 | 0.1 | 0 | 310 | 0.5 | 0.7 |
| 93 | 0.708 | 0.292 | 0 | 0 | 0 | 301 | 3.2 | 3.9 |
| 94 | 0.72 | 0 | 0.28 | 0 | 0 | 350 | 1.5 | 5.5 |
| 95 | 0.75 | 0.1 | 0.1 | 0.05 | 0 | 310 | 1.6 | 1.9 |

| | | | | | | | | |
|---|---|---|---|---|---|---|---|---|
| 96 | 0.75 | 0 | 0 | 0 | 0.25 | 350 | 6 | 3.5 |
| 97 | 0.8 | 0.1 | 0.05 | 0.05 | 0 | 310 | 0.9 | 1.1 |
| 98 | 0.8 | 0 | 0.1 | 0.1 | 0 | 310 | 0.6 | 0.9 |
| 99 | 0.8 | 0.1 | 0.1 | 0 | 0 | 310 | 1.2 | 2 |
| 100 | 0.8 | 0 | 0 | 0.1 | 0.1 | 310 | 1.6 | 1.5 |
| 101 | 0.85 | 0.05 | 0 | 0.1 | 0 | 299 | 1.6 | 3.1 |
| 102 | 0.85 | 0 | 0.05 | 0.1 | 0 | 310 | 0.4 | 0.5 |
| 103 | 0.85 | 0.1 | 0.05 | 0 | 0 | 310 | 1 | 1.4 |

**APPENDIX B: Milestones of the project**

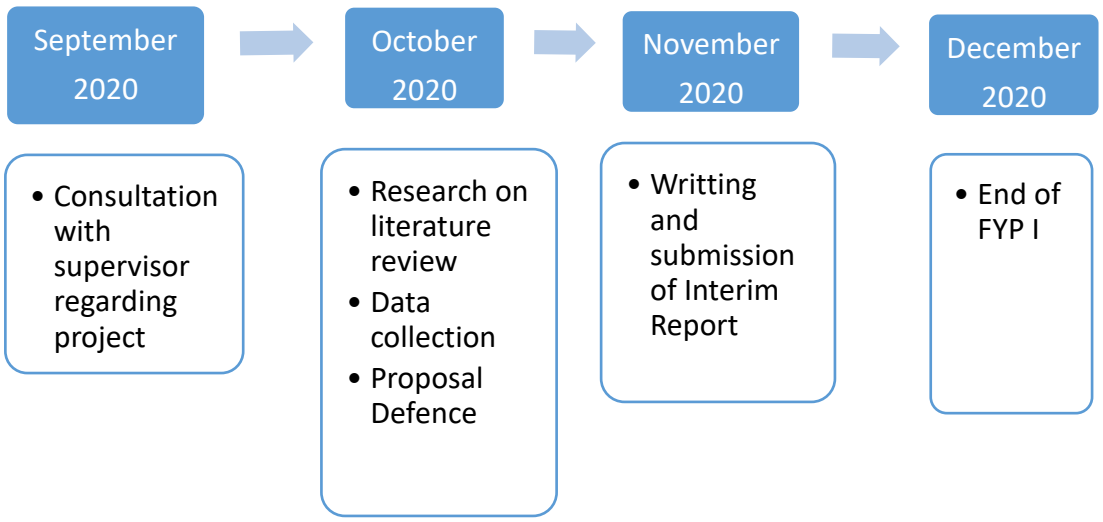


Milestone of FYP 1

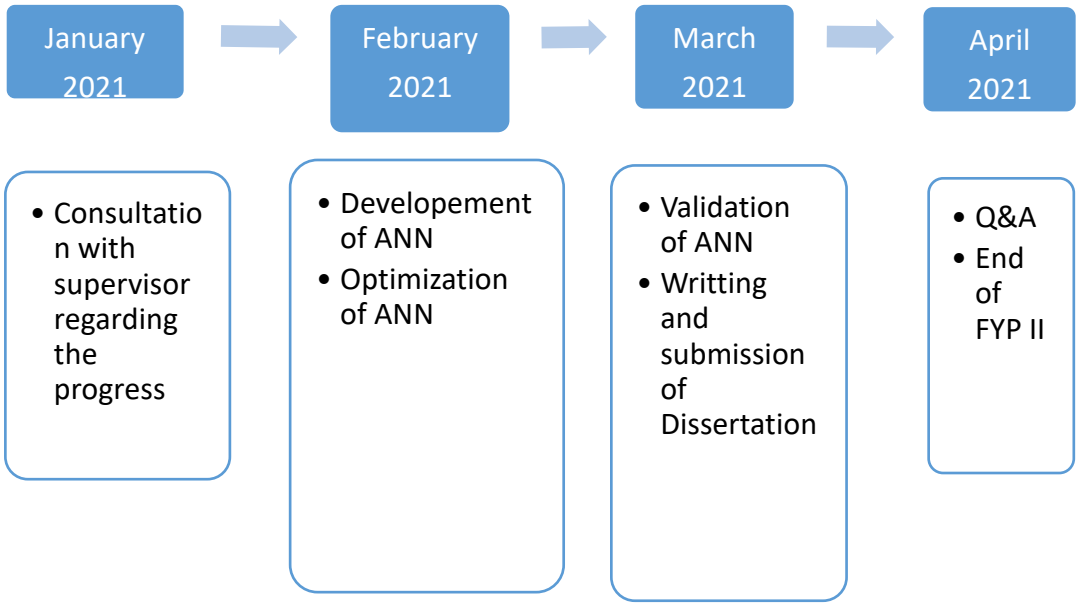


Milestone of FYP 2

## APPENDIX C: Gantt chart of the project

Artificial Neural Network Modelling of Hydrogen Storage in Metal Hydrides

Legend : Duration

| ACTIVITY | PLAN START | PLAN DURATION |
|---|---|---|
| FYP I | 1 | 12 |
| FYP II | 13 | 12 |
| Research / Literature Review | 2 | 3 |
| Proposal Defense Preparation | 5 | 2 |
| Proposal Defense Q&A | 6 | 1 |
| Data Collection | 3 | 6 |
| Develop ANN | 8 | 16 |
| Data Extration and Discussion | 10 | 14 |
| Report Writing | 2 | 22 |
| VIVA/Presentation Preparation | 22 | 3 |